Characterization of YciB, an inner membrane protein interacting with RodZ and ZipA

NOOR AFIZA BINTI BADALUDDIN

(Degree)
博士（学術）

(Date of Degree)
2015-09-25

(Date of Publication)
2016-09-01

(Resource Type)
doctoral thesis

(Report Number)
甲第6498号

(URL)
https://hdl.handle.net/20.500.14094/D1006498

博士論文

Characterization of YciB, an inner membrane protein interacting with RodZ and ZipA

RodZ および ZipA と相互作用する内膜タンパク質 YciB の解 析

平成 27 年 7 月

神戸大学大学院理学研究科

Noor Afiza Binti Badaluddin

CONTENTS

LIST OF FIGURES AND TABLES

ACKNOWLEDGEMENTS

I am grateful to my supervisor, Prof. Hiroshi Sakamoto for accepting me as his student and for his constant support.

I would also to extend my sincere gratitude to Dr. Madoka Kitakawa for her constant guidance and valuable advices throughout my research. Without her guidance and persistent help, this work and dissertation would not have been possible.

In addition, a thank you to Dr. Toshinobu Suzaki for guiding me, especially in the research using fluorescence microscope, and his valuable suggestions. I would also like to thank to Prof. Eric R. Dabbs and Prof. Kunio Inoue for critical reading for my manuscripts and thesis.

Also to be thanked are past and present members of my lab, Mio Yamamoto, Kentaro Hamamoto, Yuji Kiyota, Ngundu Ivo Woogeng and Gaochi Li for their help in my work.

Finally, I would like to express my gratitude to my husband and family in Malaysia for their unconditional love and support. Thank you very much.

SUMMARY

Cell division is a fundamental process that takes place in all living organisms. Cells of rod-shaped bacteria like *E. coli* elongate to about the twice of original length and split into two identical daughter cells. Peptidoglycan synthesis is critical for both cell elongation and division. Elongation complex containing PBP2, RodA, MreB, MreC, MreD and RodZ is important for the lateral peptidoglycan synthesis and cell-shape determination. Loss of any of these proteins leads to spherical morphology (Young, 2003; Lowe *et al*., 2004; Cabeen and Jacobs-Wagner, 2005). The cell division begins with the assembly of FtsZ into a ring-like structure (Z-ring) at the centre of the cell. Other protein components of the division machinery such as FtsA, ZipA, FtsB, FtsL FtsQ, FtsL and FtsI are recruited to the Z ring (Hale and de Boer, 1997; Hale and de Boer, 2002; Rueda *et al*., 2003). Peptidoglycan synthesis for septum formation is performed with PBP3 (FtsI) instead of PBP2. However, PBP3-independent peptidoglycan synthesis (PIPS) seems to occur preceding the invagination of cell wall and this process is directed by FtsZ and ZipA (Pichoff and Lutkenhaus, 2002). Although many of the genes that are involved in cell elongation and division have been identified, still more y-genes (function-unknown gene) seem to participate in these processes and remain to be uncovered.

In this study, I focused on *yciB*, a y-gene predicted to participate in cell division. It is a homologue of *isp*A in *Shigella flexneri* that plays a role in cell division and intracellular spreading (Mac Siomoin *et al.*, 1996). The *yciB* gene encodes a protein of 179 amino acid residues containing five transmembrane domains. Its C-terminus is located in the cytoplasm and the short N terminal region is predicted to be in the periplasm. Initially, *yciB* was identified as a gene involved in biofilm formation, which indicated that the gene might also be required for membrane integrity. Therefore, I first characterized the growth of *yciB* deletion mutant and further investigate the loss and gain effect of *yciB*. From these studies, I found that the Δ*yciB* mutant was more sensitive to the low osmolarity and shorter in the cell length compared to wild type, which seemed to indicate that the cell wall integrity of the mutant is compromised. On the other hand, the excess of YciB was toxic to the cell growth and tended to elongate the cell. Interestingly, the toxicity of excess YciB was severer in the Δ*yciB* mutant. Next, I investigated the protein-protein interaction by BACTH system and found that YciB interacts with various cell elongation and division proteins but not with MreB and FtsZ. These results obtained seemed to indicate that YciB is involved both in cell elongation and division but YciB is not a component of the elongation and the cell division complex. The observation of YciB-GFP by fluorescence microscopy was consistent with this; YciB was found throughout the cell

surface but not localized at the mid-cell. In addition, I found that the expression of full length of YciB (YciBFL) was lower than C-terminally truncated YciB derivatives, indicating that the very C-terminal peptide of 9 amino acid residues confer the toxic effect upon overexpression.

In order to confirm the previous observation (Niba *et al*., 2009) that the double deletion mutant of *ΔyciB* and *ΔrodZ* could not grow, I further examined the synthetic lethal phenotype by constructing strains that harbour Δ*yciBΔrodZ* double mutation and a chromosome integrated inducible *yciB* gene. Results obtained clearly showed that yciB was required for the growth of *ΔrodZ* mutant and furthermore the overexpressed YciB suppressed the sphere shape of *ΔrodZ* mutant. In addition, I tested the sensitivity of Δ*yciB* mutant to A22, an inhibitor of the assembly of MreB (Iwai *et al.,* 2002). The results showed that Δ*yciB* mutant was more sensitive to A22. Furthermore, only the *yciB* gene that was integrated into chromosome could partially suppress the sensitivity of the Δ*yciB* mutant. These results suggested that the well-regulated expression of YciB is important for the normal cell growth and the membrane integrity. All these results might indicate that YciB supports the function of RodZ in the lateral synthesis of peptidoglycan and MreB becomes more critical in maintaining the membrane integrity in the absence of YciB .

Finally, in order to investigate the involvement of YciB in cell division, I observed the localization of some of cell division proteins in the Δ*yciB* mutant by fluorescence microscopy. Interestingly, the localization of ZipA and ZapA were found to be abnormal in the absence of YciB. On the other hand, Δ*yciB* mutation seemed not to affect the localization of FtsZ and FtsA. ZipA and ZapA bind to ftsZ and stabilize the Z-ring. Because recent reports indicated that ZipA could have a function in the lateral peptidoglycan synthesis, especially in PIPS that occurs prior to cell division, I suspect that YciB binds ZipA and supports the movement of ZipA towards the Z-ring, thereby promoting the lateral peptidolycan synthesis in PIPS mode and the initiation of the cell division process.

Based on the results obtained, I conclude that YciB is involved in both cell elongation and cell division by cooperating with or assisting RodZ and ZipA.

1. INTRODUCTION

1.1 My personal interest in biology

All living things from a single-cell organism to higher Eukaryotes have always fascinated me. However, study more about "Life" or biology, I noticed more how they are miracle. It would be great, if I can understand the mechanisms in which they exist, stay alive and develop. Recent molecular technology seems to give an opportunity to investigate the life in the term of molecule and provided new and completely different ways of understanding the life. All living organisms begin as a single cell that divides and continues the life, where amazing events occur beyond our imagination. Even a single cell organism like bacteria seem to use various strategies, which gave me a lot of questions. It will be great to figure out how the cell grows and how it decides to divide. Here I chose to study these most important events for the life, using *Escherichia coli*, one of organisms that lead us to begin the modern biology.

1.2 *Escherichia coli*

Escherichia coli is the leading model bacterium for studying genetics, biochemistry and molecular biology. The study of E. coli that covered in many fields has increased every year due its rapid growth rate, simple nutritional requirements and genetic manipulation. However, despite the impressive of the available data from several decades of study, the details of gene regulation and many mechanisms in *E. coli* are still far from being complete. Therefore, this study was conducted to reveal more information about this organisms especially in cell elongation and division processes.

E. coli a gram negative bacterium that is found in the environment, foods, and intestines of people and animals. *E. coli* belongs to *Enterobacteriaceae* in ϒ-proteobacteria class, is a facultatively anaerobic, and rod-shaped with measurement approximately 0.5 μm in width and 2 μm in length (Figure 1(a)). *E. coli* was first discovered in the human colon in 1885 by German bacteriologist Theodor Escherich. Nowadays, more than 700 serotypes of *E. coli* have been identified. The "O" and "H" antigens on the surface of bacteria and their flagella distinguish the different serotypes. Most *E. coli* strains are harmless, but some serotypes can cause serious food poisoning in their hosts.

E. coli has been studied as a model organism in microbiological studies for decades. A comparison to genome annotations of other model organisms shows that the *E. coli* genome was most extensively analyzed and the cellular function has experimentally been attributed to

the largest number of genes in both relative and absolute terms: 2941 (66%) for *E. coli*, 2319 (37%) for *Saccharomyces cerevisiae*, 1816 (5%) for *Arabidopsis thaliana*, 1456 (4%) for *Mus musculus* and 614 (4%) for *Drosophila melanogaster*. Of the 4460 *E. coli* genes, in addition, EcoCyc assigns biochemical functions to 76% of all genes (Karp *et al.*, 2007). The genome of *E. coli* K-12 with 4,639,221 base pairs was completely sequenced in 1997 and predicted to encode 4288 protein-coding genes, among which 38 percent had no attributed function (Blattnerr *et al.*, 1997). The largest family of paralogous genes is ABC transporter with 80 transporter proteins. Then, the complete genome sequence of enterohaemorrhagic *E coli* O157:H7 strain EDL933 has been reported by Perna *et al.* (2001). This genome sequence provided an important information for comparing the pathogenic *E. coli* with the harmless one. More recently, several resources have been constructed such as ORF plasmid clone library (A Complete Set of *E. coli* K-12 ORF Archive Library, ASKA) (Kitagawa *et al.*, 2005) and a single deletion library of predicted ORFs (Keio Collection) (Baba *et al.*, 2004) to facilitate the study of this organism. From the construction of Keio Collection they found that 303 genes are essential (including 37 genes of unknown function) (Figure 1(b)). Nowadays, there are many techniques available to identify the function of gene such as transposon mutagenesis, transcriptional analysis, i*n vivo* and *in vitro* protein interaction and many more. However, the precise functions of many genes still remain uncovered.

1.3 *E. coli* cell elongation

Bacteria exist in variety of shapes and required an intact peptidoglycan to maintain the defined cell shape. The thickness of peptidoglycan in Gram-negative bacteria is 3-6 nm, which is likely a single layer and thinner than peptidoglycan in Gram-positive bacteria (Vollmer and Seligman, 2010). Bacterial peptidoglycan protects the cell from internal pressure or harsh environmental condition. Peptidoglycan synthesis is a basic process for cell growth and division. In cell cycle, the peptidoglycan of the murein sacculus elongates by incorporating newly synthesized single glycan strands into the existing sidewall and making intercalation between them. Cell division is preceded by formation of a transverse septum at the center of the cell, followed by the splitting of the septum to form the poles of the daughter cells (Uehara and Park, 2008).

(a)

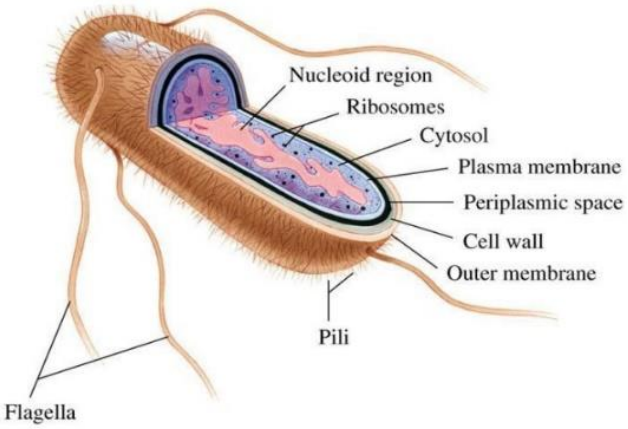

(b)

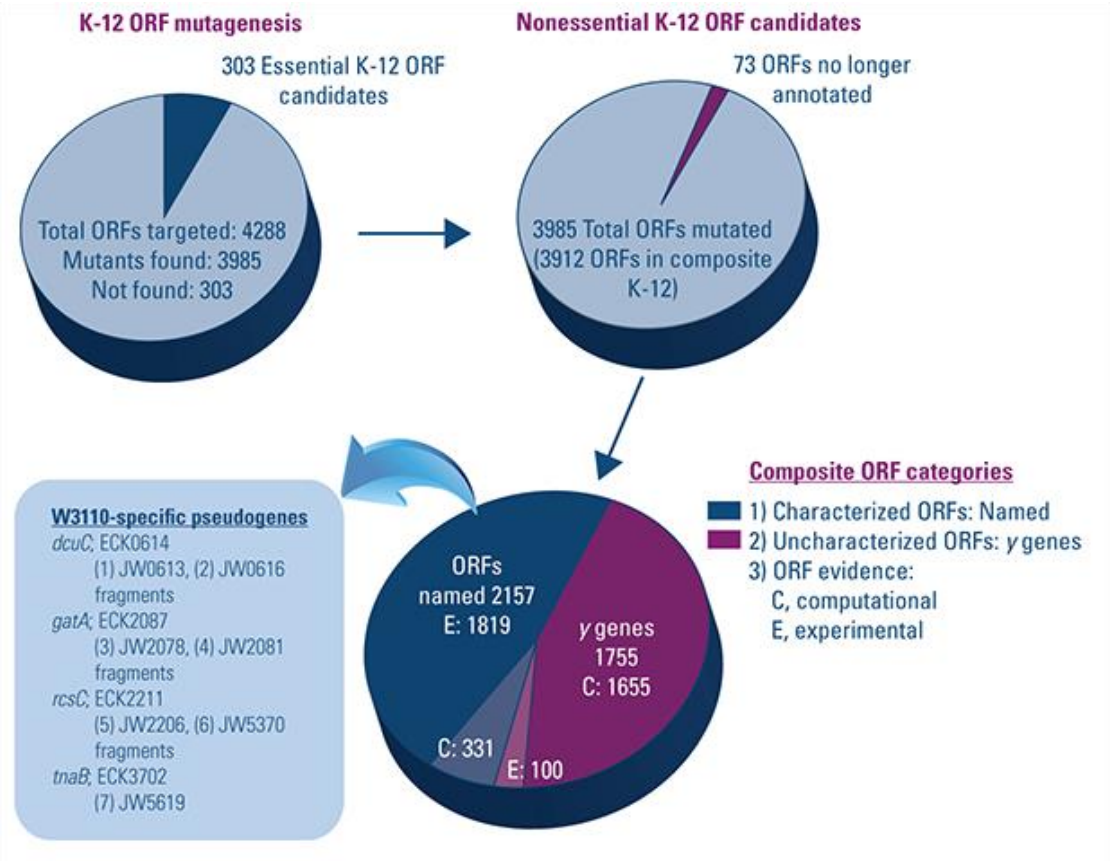

Figure 1: (a) Structure of *E. coli*. (b) Construction of KEIO collection and classification of genes in *E.coli* K12. (adopted from Baba *et al.*, 2004).

1.3.1 Peptidoglycan synthesis

Peptidoglycan of gram-negative bacteria is placed in the periplasm and essential for cell wall integrity. The peptidoglycan is made of glycan chains of alternating N-acetylglucosamine and N-acetylmuramic acid cross-linked by short stem peptides attached to the N-acetylmuramic acid (Vollmer *et al.*, 2008). There are many enzymes involved in the synthesis of peptidoglycan, from the synthesis of precursor to the formation of peptidoglycan succulus (Figure 2). Key intermediates of precursor synthesis are the nucleotide activated amino sugars uridindiphosphate-N-acetyl-glucosamine (UDP-GlcNAc) and uridindiphosphate-N-acetyl-muramic acid (UDP-MurNAc). The peptide side chain (L-Ala, D-Glu, m-A_2pm and D-Ala-D-Ala dipeptide) is formed at the lactyl group of UDP-MurNAc by ATP-dependent ligases MurC, MurD, MurE and MurF (Vollmer and Bertsche, 2008).

Meanwhile, MreB forms filaments and interacts with the conserved inner-membrane proteins MreC, MreD, RodA and RodZ (Kruse *et al.*, 2005; Shiomi *et al.*, 2008), as well as with the lipid II synthesis enzymes MraY and MurG, to form the elongation complex prior to direct the peptidoglycan elongation synthesis (Mohammadi *et al.*, 2007). MraY attached a C_{55}-polyisoprenoid carrier to form Lipid I (undecaprenyl pyrophosphoryl-MurNAc-peptapeptide), followed by the addition of GlcNAc from UDP-GlcNAc to lipid I to form Lipid II that catalyzed by MurG (Vollmer and Bertsche, 2008). This elongation complex is very important for *E. coli* to determine rod-shape morphology. Inactivation of any of these genes result in sphere-shaped bacteria. (Lowe *et al.*, 2004; Kruse *et al.*, 2005). The rod-shaped bacterium, *Caulobacter crescentus* produces an additional shape-determining protein called *crescentin*, which is responsible for its characteristic curved morphology (Møller-Jensen and Lowe, 2005).

Next, the precursor lipid II is flipped across from cytoplasmic to the periplasmic by flippases and murein sacculus are synthesized by incorporating lipid II precursor. Murein synthesis, that is, the polymerization of glycan strands (transglycosylation) and the cross-linking between glycan chains (transpeptidation) are catalyze by PBPs, which act as glycosyltransferase (GTase) or/and tranpeptidase (TPase). Class A PBPs like PBP1A and PBP1B are bifunctional enzymes with highest murein synthesis activity in the cell (Vollmer and Bertsche, 2008). A double deletion of these enzymes is lethal and mutants lacking PBP1B are more sensitive to β-lactam antibiotics than mutants without PBP1A (Spratt and Jobanputra, 1977; Yousif *et al.*, 1985). In addition, the essential protein penicillin-binding protein 2 (PBP2) function as TPase to form cross-linkages in peptidoglycan during elongation. *E. coli* PBP2 is similar to *Staphylococcus aureus* PBP3 (Ishino *et al.*, 1986).

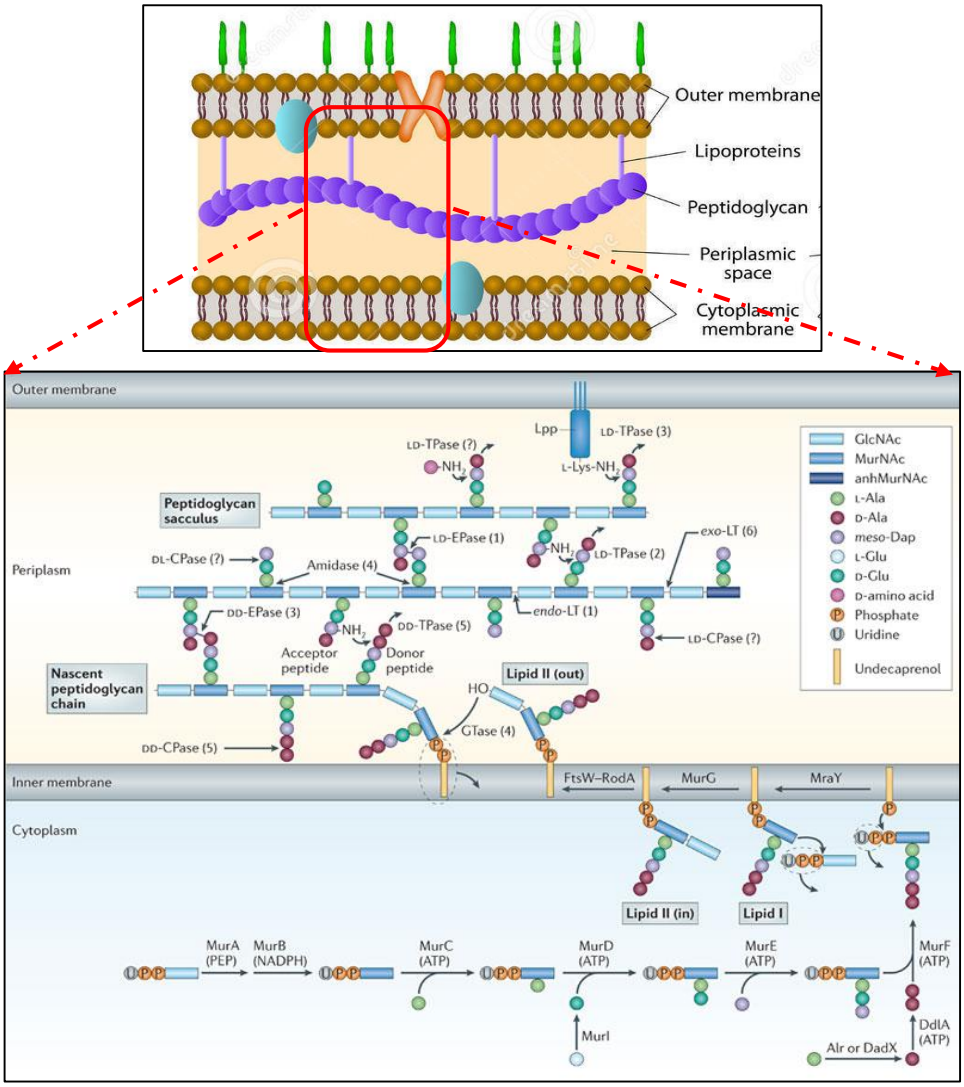

Figure 2: The structure of E. coli cell wall (upper) and the synthesis of peptidoglycan (below) (Typas *et al.*, 2012).

The synthesis of new peptidoglycan strand require many synthetic and degrading enzymes. Precursors are synthesized in the cytoplasm, linked to the transport lipid and flipped across the inner membrane by FtsW-RodA. A glycosyltranferase (GTase) catalyzes the polymerization of a nascent peptidoglycan chain from lipid II precursor at the inner membrane, followed by attachment of the new chain to the sacculus by a DD-transpeptidase (TPase). Peptides are trimmed by carboxypeptidase (CPase) and crosslinks are cleaved by endopeptidases (EPase). Amidases remove peptides from glycan chains, and exo- or endo-specific lytic transglycosylases (LTs) cleave in the glycan chain to form 1,6-anhydro-N-acetylmuramic (anhMurNac) acid residues, which are the hallmark of glycan chain ends. LD-TPase are responsible for the formation of LD-crosslinks, the attachment of the major outer-membrane lipoprotein (Lpp), which is anchored in the outer membrane, and the binding of unusual D-amino acids.

1.3.2 RodZ, a rod shape determinant protein

RodZ (Require an overdose of FtsZ) is an important protein for cell shape maintainance and peptidoglycan synthesis (Shiomi *et al.*, 2008; Bendezú *et al.*, 2009; Niba *et al.*, 2010). This membrane protein is well conserved among bacterial species, both in Gram negative and Gram positive bacteria. *rodZ* encodes for an inner membrane protein of 337 amino acids and posseses a Cro/Cl- type DNA-binding Helix-turn-Helix (HTH) domain (1-84 a.a), juxta membrane region (84-110 a.a), a transmembrane domain (111-133 a.a) and periplasmic domain (134-337 a.a). A deletion analysis showed that the cytoplasmic domain of RodZ is required for the formation of RodZ helices and its HTH motif was found to be important for interaction between MreB and RodZ (Bendezu *et al.*, 2009; van den Ent *et al.*, 2010). A Δ*rodZ* mutant forms sphere cell and shows defective in peptidogycan synthesis. Furthermore, the mutants lacking *rodZ* grows slower than wild type and more sensitive to low osmolarity (Niba *et al.*, 2010).

1.4 *E.coli* cell division

Gram-negative bacteria like *E. coli* employ a constrictive mode of cell division, where septal peptidoglycan synthesis and septum invagination occur simultaneously during division (Egan and Vollmer, 2013). Before the cell division to occur, the cell must replicate its DNA and segregate these copies to opposite ends of the cell. Then, the cell division begins with formation of FtsZ ring at the midcell. The localization of FtsZ-ring is regulated by Min system consisting of MinC, MinD and MinE. MinC and MinD oscillate from pole to pole, inhibiting the assembly of FtsZ and preventing the formation of inappropriate division sites at the cell pole. Meanwhile, the suppression of MinC/D inhibition at the mid-cell is facilitated by an additional protein, MinE. (de Boer *et al.*, 1991; Hu *et al.*, 1999; Shih *et al.*, 2003; Hsieh *et al.*, 2010). In *Bacillus subtilis*, the Min system and DivIVA, together with EzrA protein prevent the assembly of Z rings near the poles (Edwards and Errington, 1997; Singh *et al.*, 2007). The assembled FtsZ ring recruits the other division proteins, such as FtsA, ZipA, and PBP3 to the future division site. Another protein, ZapA and ZapB have also been shown to be an FtsZ binding protein that can stabilise and polymerize FtsZ-ring (Mohammadi *et al.*, 2009). FtsZ polymerization enhanced the peptidoglycan synthesis at the division site with PBP3, a core member of the cell division complex “divisome”. It is recruited to the septum by the lipid II flippase FtsW, and interacts with the FtsQLB complex, PBP1B and FtsN. PBP3 together with at least nine other cell divisiare required for the septum formation, and in the absence or inactivation of these proteins, the septation ceases and filamentous cells are formed (Addinall

et al., 1996; Chen *et al.*, 1999; Hale and de Boer, 1997; Vollmer and Bertsche, 2008). The divisome complex redirects cell wall growth and prevents damage to the DNA while the cell envelope invaginates (Nanninga, 1991). The order and timing of all these processes are tightly controlled. Then, the cell divides into two equivalent daughter cells.

The structure and function of protein components for the cell division and cell elongation complexes have been investigated in various ways. However, relatively little is known about how the cell shifts from the elongation to the cell division stage. Previously it was reported that prior to the septum formation a distinct peptidoglycan synthesis occurs at the mid-cell, which is directed by FtsZ and driven by PBP2 instead of cell-division specific transpeptidase PBP3 (Wientjes & Nanninga 1989; Varma *et al.* 2007). This process called PIPS (PBP3-*i*ndependent *p*eptidoglycan *s*ynthesis) represents the earliest detectable signature of the transition from elongation to division. Recently, it was found that this PIPS also requires ZipA for elongation at the division site (Potluri *et al.* 2012).

The cell division process in *E. coli* has extensively been studied for decades, however details are still unclear. Recent investigations identified few *y*-genes involved in cell division in *E.coli* such as YmgF, YcbW (known as ZapC) and YacF (known as ZapD) (Karimova *et al.*, 2009; Durand-Heredia *et al.*, 2011; Hale *et al.*, 2011). However, the precise role and mechanism in which they play are not yet fully understood. Furthermore, it is not clear how the cell determines and senses the defined cell length during cell elongation and proceeds to the division process and form two daughter cells.

1.4.1 ZipA, a Z-ring stabilizer

ZipA (FtsZ interacting protein A) is a cell division protein with 328 amino acid residues of estimated molecular weight 36.5 kDa. This gene is predicted to be a bitopic membrane with four domains: an N-terminal transmembrane anchor, a charged domain, a domain enriched in proline and glutamine and a C-terminal globular domain. ZipA is recruited to the division site by FtsZ to form the Z-ring during cell division (Hale and de Boer, 1997). The recruitment of ZipA to the Z-ring is independent of the other FtsZ-interacting protein FtsA (Hale and de Boer, 1999). It has been observed that the FtsZ-ring can form while either ZipA or FtsA protein is absent, however, FtsZ-ring cannot form if both of proteins are absent (Pichoff and Lutkenhaus, 2002). ZipA homologues are not found outside the γ-proteobacterial family, but the requirement for ZipA can be bypassed completely by a single alteration in a conserved residue

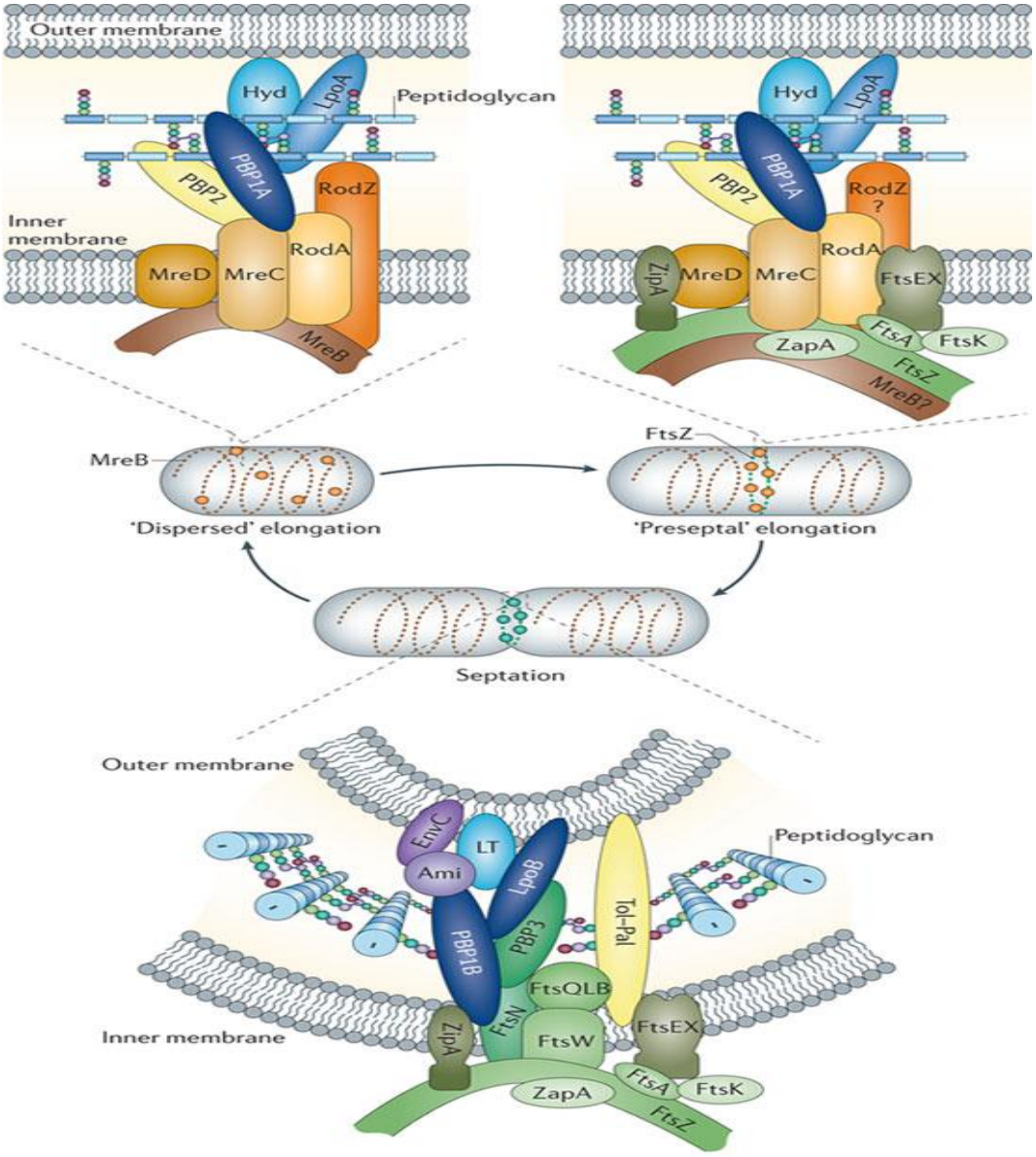

Figure 3: Cell elongation and division processes.

The model with predicted proteins that involved in cell elongation and division processes (Typas *et al.*, 2012).

of FtsA (Geissler *et al.*, 2003). In addition, FtsZ binds directly to the C-terminal globular domain of ZipA, named the FtsZ binding (FZB) domain and ZipA also induces bundling of FtsZ protofilaments (Hale *et al.*, 2000). ZipA has been estimated to be present at 1000-1500 copies in the cell. This indicates that a limited number of the FtsZ molecules will be interacting with either ZipA or FtsA. An overproduction of ZipA might cause a decrease in the concentration of FtsZ that is not bound to ZipA and led to the formation of filamentous cells due to the division block. However, overexpression of FtsZ can relieved the division block imposed by a high level of ZipA (Hale and de Boer, 1997). Recently, it was found that ZipA was also required for cell elongation at the division site that mediated by PIPS (Potluri *et al.*, 2012) and a mutation in the promoter region of ZipA suppresses the sphere shape of Δ*rodZ* mutant (Shiomi and Niki, 2013). These investigations further suggest that this protein might have extra function. Nowadays, an increasing number of proteins are identified as moonlighting proteins or multifunctional proteins (Huberts and van der Klei, 2010).

1.5 YciB, a function- unknown protein

As described above, more than 30% of *E. coli* genes still remain function-unknown and these genes are referred as hypothetical gene or "y-genes", because they were temporarily named after the letter "y". Traditional gene names derive from a phenotype mnemonic, or from the identification of a gene based on the protein or RNA product it makes. For example, *ftsA* refers to the characterization of the protein which are filamentation, temperature sensitive, while *ssrA* is for "small stable RNA". For y gene nomenclature, the next two letters was given systematically depends on the position of the gene on the standard map of *E. coli* K-12 strain MG1655. The uppercase letter was given to distinguish the gene with other genes in the region (*Ecoli*Wiki).

The gene *yciB,* (alternate name; *ispZ*-Intracellular Septatation Protein), is a gene unknown-function that maps at 28 minutes. *yciB* encodes an inner membrane protein of 179 amino acid residues containing five transmembrane domains. Its C-terminus is located in the cytoplasm and the short N-terminal region in the periplasm (Figure 3). YciB is a homolog of *ispA* in *Shigella flexneri*, the gene found responsible to the failure of cell division within the host epithelial cytoplasm. A mutant of *ispA* has led to the formation of long filamentous cells lacking septa, which are unable to spread intercellularly (Mac Siomoin *et al.*, 1996). Furthermore, the screening of Keio collection also identified *yciB* as a gene involved in biofilm formation (Niba *et al.*, 2007), which indicated that the gene might contribute to maintain the

membrane integrity. However, no observation and examination was reported that indicates that *yciB* is involved in cell elongation or division in *E. coli.* Therefore, I applied several methods that might provide data for this function-unknown gene.

Synthetic phenotype analysis is one of the effective methods to investigate the genetic interaction between an unknown gene and known genes and might indicate functional relationship between tested genes. Synthetic phenotype will be obtained if a combination of mutations in two or more genes confers detectable phenotype such as cell death or adversed cell growth. The synthetic lethal interactions occur between two genes or pathways that can compensate for each other because of inherent functional redundancy or when the loss of one gene results in converting the other gene to essential, although it may share no functional similarity with the lost gene, such as toxic and anti-toxic genes (Nijman, 2011). Recently, protein-protein interaction analysis was widely used to identify or predict the function of protein in question, because proteins tend to interact with other proteins functioning in the same cellular process. Nowadays, there are various methods either *in vivo* or *in vitro* to study the interaction. Two-hybrid systems are extremely powerful methods for detecting protein-protein interactions in vivo. Two-hybrid system was first developed with yeast *Saccharomyces cerevisiae* (Field and Song, 1989), which is using the GAL4 transcriptional activator of the yeast *S. cerevisiae*. More recently, Bacterial Two Hybrid system (BACTH) has been approached and applied for protein interaction in *E. coli* (Karimova et a., 1998). On the other hand, various *in vitro* methods are applied to examine the direct protein-protein interactions. Common *in vitro* methods are co-immunoprecipitation and pull-down assays with special tag such as 6xHis tag or FLAG (Hochuli *et al.*, 1988; Thomas *et al.*, 1988).

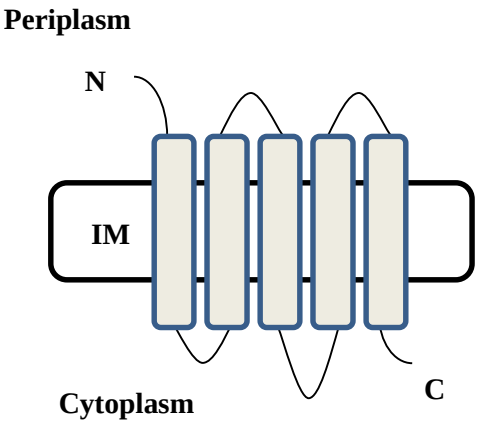

Figure 4: The structure of YciB protein.

1.6 Objectives of this study

Cell elongation and cell division are essential processes for the bacterial propagation. As described before, the *yciB* was identified as a gene involved in biofilm formation through the screening of Keio collection. Furthermore, the Δ*yciB*Δ*rodZ* double mutations caused synthetic lethality (Niba *et al.*, 2007). These investigations indicated that *yciB* plays a role in the synthesis of peptidoglycan and the cell shape determination. On the other hand, the homology to *ispA* suggested the involvement of the *yciB* in cell division. Therefore, the objective of this study is to investigate the mechanisms in which *yciB* participates in cell elongation and cell division and to obtain clues to elucidate how bacteria connect these fundamental processes. In this work I have employed the following strategies:

a) Characterize the Δ*yciB* mutant (growth property and cell morphology).

b) To examine the protein-protein interactions between YciB and cell elongation and division proteins by BACTH system.

c) To investigate the genetic relation with genes involved in cell elongation and cell division.

d) To investigate the cellular localization of YciB and other proteins involved in cell division in the Δ*yciB* mutant.

2. MATERIALS AND METHODS

2.1 *E coli* strains, plasmids and synthetic primers used in this study

E. coli K12 strains and plasmids used in this work are listed in Table 1 together with primers used in PCR amplification. Δ*yciB*::*Kan*^{R} and Δ*rodZ*::*Kan*^{R} mutations were introduced from JE1246 and JE2500 of the Keio collection (Baba *et al.,* 2006), respectively, into indicated strains by P1kc mediated transduction. Elimination of the kanamycin resistant cassette was performed as previously described (Datsenko and Wanner, 2000; Niba *et al.,* 2010). The inducible *yciB* (P_{ara}-*yciB*) together with *araC* and *bla* (Amp^R) were transferred from plasmid pBADs-*yciB* and integrated into the chromosome near the *att*λ using λInCh as previously described (Niba *et al.,* 2010; Boyd *et al.,* 2000).

Table 1: *E coli* strains, plasmids and primers used in this study.

	Genotype/Features or primers[a]	**Source or Reference**
E.coli strains		
XL1	F$^-$[*proAB+,laqIq, lacZDM15::Tn10(tetr)*], *hsdR17, supE44, recA1, endA1, gyrA46, thi, relA1, lac*	Stratagene, Laboratory stock
JE8471	F$^-$, *DE(cya)854, trp, his, ilv*	National BioResource Project
BW25113	F$^-$, *rph-1, DE(rhaBAD)568, DE(araBAD)567, DElacZ4787, hsdR514, rrnB*	Baba *et al.*, 2006
KR0401	a derivative of BW25113	Niba *et al.*, 2007
KR1411	KR0401Δ*yciB::Kan*^{R} [b]	This study
KR1412	KR0401Δ*yciB::Kan*^{S} [c]	This study
KR1421	KR0401Δ*rodZ: Kan*^{R} [b]	This study
KR1431	KR0401 *attλ*::(p_{ara}-*yciB, araC ,bla*) [d]	This study
KR1432	KR0401 *attλ*::(p_{ara}-*yciB, araC ,bla*) [d], Δ*yciB:: Kan*^{R} [b]	This study
KR1433	KR0401 *attλ*::(p_{ara}-*yciB, araC ,bla*) [d], Δ*rodZ:: Kan*^{R} [b]	This study

KR1434	KR0401 *attλ*::(p_{ara}-*yciB, araC ,bla*) [d], Δ*yciB:: Kan*^{S} [c], *ΔrodZ:: Kan*^{R} [b]	This study
KR1435	KR0401 *attλ*::(p_{ara} *araC ,bla*) [d], Δ*yciB:: Kan*^{R} [b]	This study
KR1436	KR0401 *attλ*::(p_{ara}-*yciB-gfp, araC ,bla*) [d]	This study
P773	CH3 *λ bla lacI*^{q} P_{lac}*::zipA-gfpS65T*	Hale and de Boer, 1997
P774	CH3 *λ bla lacI*^{q} P_{lac}*::gfpmut2-t-ftsA*	Hale and de Boer, 1999
P789	CH3 *λ bla lacI*^{q} P_{lac}*::gfpmut2-t-ftsZ*	Hale and de Boer, 1999
Plasmids		
pCA24N-*zipA*	*zipA-GFP* tagged, Cm^{R}	Kitagawa *et al*., 2005
pCA24N-*zapA*	*zapA-GFP* tagged, Cm^{R}	Kitagawa *et al*., 2005
pCA24N-*yciB*	*yciB-GFP* tagged, Cm^{R}	Kitagawa *et al*., 2005
pBAD322s	derivative of pBAD322, Ap^{R}	Niba *et al*., 2010
pBAD322s-*yciBFL*	ggaattcATGAAGCAGTTTCTTGATTTTTTACC ctaggcctGGATTTATCTTCCTGCGGC	This study
pBAD322s-*yciB170*	ggaattcATGAAGCAGTTTCTTGATTTTTTACC gcgcatgcTGCATTCGAGCTCGGTACC *yciB170* derived from pUT18-*yciB170*	This study
pBAD322s-*yciB147*	ggaattcATGAAGCAGTTTCTTGATTTTTTACC gcgcatgcTGCATTCGAGCTCGGTACC *yciB147* derived from pUT18-*yciB147*	This study
pBAD322s-*yciB118*	ggaattcATGAAGCAGTTTCTTGATTTTTTACC gcaggcctCAGCTTCGACCATACCGGTTG	This study
pBAD322s-*yciB48*	ggaattcATGAAGCAGTTTCTTGATTTTTTACC gcaggcctCTCAACCTTACGAAAGCGAACC	This study
pBAD322s-*malG*	gctctagaGGCAATGGTCCAACCGAAAT gcgcatgc ACCTTTCACACCACCTGCC	This study
pUT18	BACTH vector, Km^{R}	Karimova *et al*., 1998

pKT25	BACTH vector, Ap^R	Karimova *et al*., 1998
pKnT25	BACTH vector, Ap^R	Li *et al*., 2012
pUT18-*yciBFL*	gctctagaGAAGCAGTTTCTTGATTTTTTACC cgggatccAGGATTTATCTTCCTGCGGC	This study
pUT18-*yciB170*	gctctagaGAAGCAGTTTCTTGATTTTTTACC cGGTACC CGGTAGATATAGATACCGCTTAA	This study
pUT18-*yciB147*	gctctagaGAAGCAGTTTCTTGATTTTTTACC gcggtaccTTGACCCAAATATTTTGCGGC	This study
pUT18-*yciB118*	gctctagaGAAGCAGTTTCTTGATTTTTTACC gcggtaccTTCAGCTTCGACCATACCGGTTG	This study
pUT18-*yciB48*	gctctagaGAAGCAGTTTCTTGATTTTTTACC gcggtaccTTCTCAACCTTACGAAAGCGAACC	This study
pUT18-*zipA*	gctctagaGATGCAGGATTTGCGTCTGATA gcgaattcGCGTTGGCGTCTTTGACTTC	This study
pKnT25-*yciBFL*	*yciBFL* derived from pUT18-*yciBFL*	This study
pKnT25-*yciB170*	*yciB170* derived from pUT18-*yciB170*	This study
pKnT25-*yciB147*	*yciB147* derived from pUT18-*yciB147*	This study
pKnT25-*yciB118*	*yciB118* derived from pUT18-*yciB118*	This study
pKnT25-*yciB48*	*yciB48* derived from pUT18-*yciB48*	This study
pKT25-*mreB*		Li *et al*., 2012
pKT25-*mreC*		Li *et al*., 2012
pKT25-*mreD*		Li *et al*., 2012
pKT25-*murG*		Li *et al*., 2012
pKnT25-*rodA*		Li *et al*., 2012
pKT25-*rodZ*		Li *et al*., 2012
pKNT25-*ftsA*	gctctagaGATCAAGGCGACGGACAG gcggatccAACTCTTTTCGCAGCCAACT	This study
pKT25-*ftsB*		Li *et al*., 2012
pKT25-*ftsL*	gc*tctaga*GATCAGCAGAGTGACAGAAGCT c*ggtacc*TTTTGCACTACGATATTTTCTTG	This study
pKT25-*ftsQ*	gctctagaGTCGCAGGCTGCTCTGAA gcgaattcTGTTGTTCTGCCTGTGCCTGA	This study
pKnT25-*ftsZ*	gctctagaGTTTGAACCAATGGAACTTACC cgggatccTCAGCTTGCTTACGCAGGAAT	This study

pKnT25-*zapA*	gctctagaGTCTGCACAACCCGTCGATA gcggtaccTCAAAGTTTTGGTTAGTTTTTT	This study
pKnT25-*zipA*	gctctagaGATGCAGGATTTGCGTCTGATA gcgaattcGCGTTGGCGTCTTTGACTTC	This study
pKnT25-*malF*	gctctagaGGATGTCATTAAAAAGAAACATTGG gcggtaccTCAAACTTCATTCGCGTGGCT	This study
pKnT25-*malG*	gctctagaGGCAATGGTCCAACCGAAAT gcggtaccACCTTTCACACCACTGCCGT	This study

[a] Used to amplify the indicated genes. Lower case letters indicate sequences of restriction enzyme sites appended to facilitate the cloning.

[b] Kan^R : deletion mutation containing kanamycin resistant cassette was introduced by p1kc transduction from relevant strain in Keio collection.

[c] Kan^S: Kan^R cassette was removed by pCP20 (Datsenko and Wanner, 2000), leaving a Frt scar.

[d] *attλ*::(p_{ara}-*yciB, araC ,bla*): genes on plasmid pBADs-*yciB* were integrated near *attλ* site of the chromosome using λInCh (Boyd *et al.*, 2000).

2.2 Growth media and antibiotics

Bacteria were routinely grown in LB media (0.5% NaCl) at 37°C unless indicated otherwise. Antibiotics ampicillin (100 μg/ml), kanamycin (40 μg/ml) and chloramphenicol (40 μg/ml) were added when required. A22 (Calbiochem) dissolved in water (2 mg/ml) was added to agar plates to give the indicated concentration. Plates were used in 24 hours because A22 is unstable in the rich medium. Minimal AN medium was prepared as described (Davis and Mingioli 1950). P1kc phage was propagated on LC agar plate (1 % Bacto-tryptone, 0.5 % yeast extract, 0.25 % NaCl and 1 % Bacto-agar) with Top agar (1 % Bacto-tryptone, 0.5 % yeast extract, 0.05 % NaCl, 2 mM NaOH and 0.5 % Bacto-agar (Difco)) basically according to Miller (1972).

2.3 Preparation of plasmid DNA

1.5 ml cells from an overnight culture were transferred to an Eppendorf tube, centrifuged at 15,000 rpm for 30 sec and the supernatant discarded. The tube was towel-dried and 200 ml of STET containing lysozyme (0.25 mg/ml) was added. The mixture was vortexed

and boiled for 1min. Immediately after that, it was centrifuged at 15,000 rpm for 5 min and the precipitate removed with a toothpick. 8 ml of 5% acetyl trimethyl ammonium bromide (CTAB) was added and again centrifuged at 15,000 rpm for 5 min. 300 ml of 1.2M NaCl was added and then well-mixed before adding 750 ml 100% ethanol. The mixture was centrifuged again at 15,000 rpm for 5 min and the supernatant discarded. 500 ml 70% ethanol was added and the plasmid DNA was collected by centrifugation at 15,000 rpm for 5 min. The ethanol was removed by aspiration or drying at 42 ^{o}C. After which 30 ml sterilized H_2O was added and then stored at –20 ^{o}C until needed.

Solution:

STET buffer:

Sucrose	8 %
TritonX-100	0.1 %
EDTA	50 mM
Tris-HCl (pH 8.0)	50 mM

2.4 Construction of S-tagged fusion proteins

All plasmids containing the S-tagged protein genes were constructed using pBADs vector derived from pBAD322 (Cronan, 2006). The S-tag carrying sequence from pSH-*Leu* (Gan *et al.*, 2002) was ligated into the Sph1 and Hind111 site of the MCS of pBAD322. To construct tagged proteins, the DNA fragments harboring ORF of respective genes without the termination codon were PCR amplified from the respective plasmid DNA (pUT18 clones) using appropriate primers (Table 1) to add restriction enzyme sites. They were then inserted into the multi-cloning site of pBADs in frame.

2.5 Construction of BACTH clones

Bacterial two hybrid analysis was performed essentially as described (Karimova *et al*., 1998). The genes encoding the two proteins of interest (X or Y) were amplified from either chromosomal DNA or from the relevant plasmid by PCR using appropriate primers (Table 1) and sub-cloned into pKT25 (or pKNT25) and pUT18 vectors in frame with the T25 and T18 fragment open reading frames by using standard molecular biology techniques.

BACTH vector (http://www.euromedex.com) (Figure 5)

pUT18

pUT18 is a derivative of the high copy number vector pUC19, expressing an ampicillin resistance selectable marker, and encodes the T18 fragment (amino acids 225 to 399 of CyaA) that is expressed under the transcriptional control of a lac promoter. The T18 open reading frame lies downstream of a MCS with 9 unique restriction sites. This plasmid is designed to express chimeric proteins in which a heterologous polypeptide is fused to the N-terminal end of T18.

pKT25

pKT25 encodes the T25 fragment (corresponding to the first 224 amino acids of CyaA) that is expressed under the transcriptional control of a *lac* promoter. The pKT25 vector is a derivative of the low copy-number plasmid pACYC184, expressing a kanamycin resistance selectable marker. A multi-cloning site sequence (MCS) is inserted at the 3' end of T25 to allow construction of in-frame fusions at the C-terminal end of the T25 polypeptide.

pKnT25

Plasmid pKnT25 was constructed from pKTop (Karimova *et al*., 2009) by replacing the region containing PhoA and LacZ fragments of the vector with the fragment coding for T25 using In-Fusion system (ClonTech/Takara Bio). The T25 fragment was amplified by PCR using pKT25 as template and primers, pKTop-T25-5 (GATCCCCGGGTACCGAGCTCGAATTCAATGACCATGCAGCAATCGC) and pKTop-T25-3-rv (AGATTGTACTGAGAGTGCACTTATATCGATGGTGCAGCCCGCCGCGTGCG).

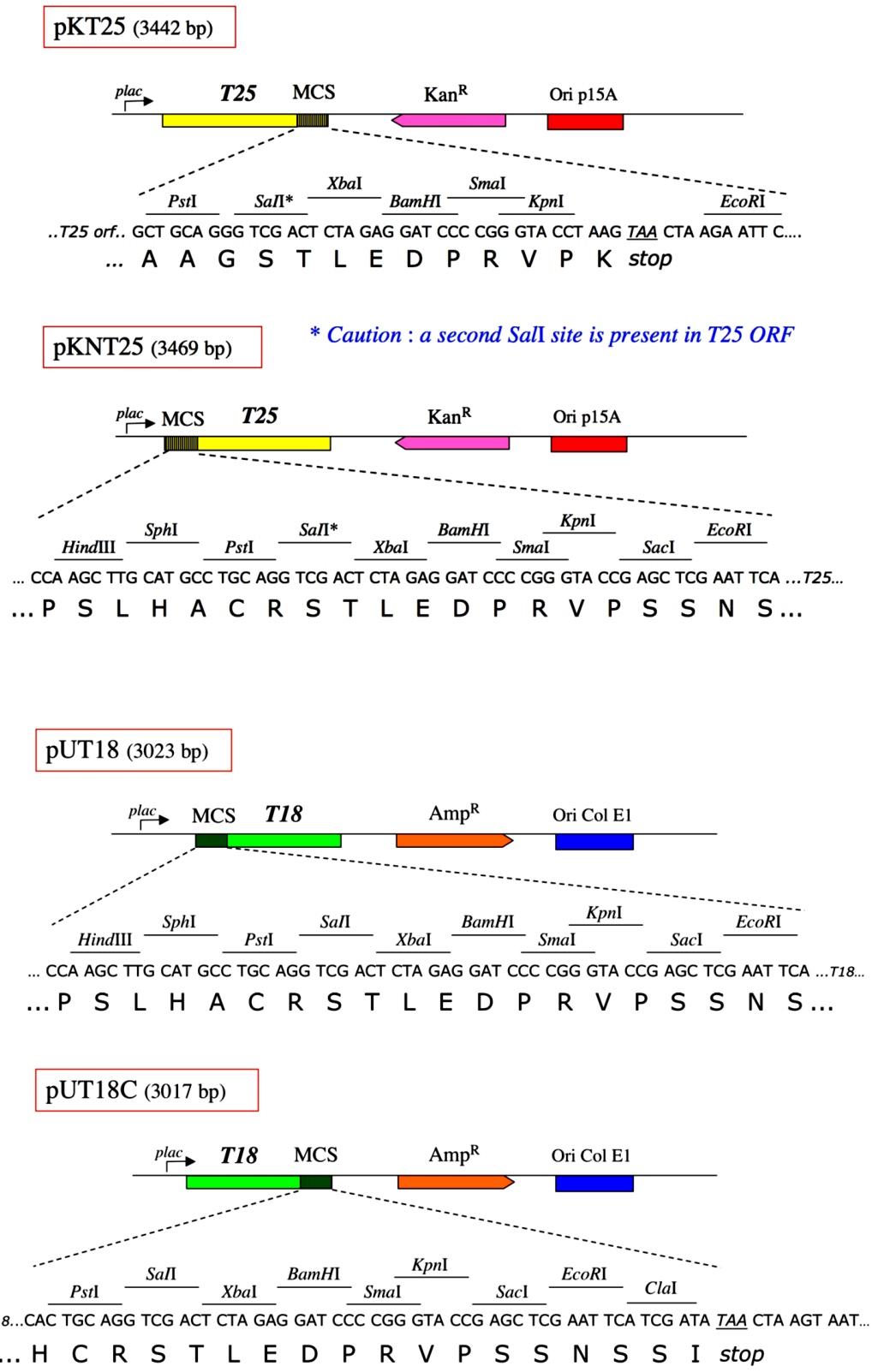

Figure 5: BACTH plasmid maps.

2.6 Transformation of plasmid DNA into competent cells ($CaCl_2$ method)

5ml of LB medium (with antibiotics when necessary) was inoculated with 0.1 ml of overnight culture of cells to be transformed and incubated at 37ºC until the OD_{600} was approximately 0.5. The cells were harvested by centrifuging at 3,000 rpm for 10 min at 4ºC, and the supernatant was discarded. Cells were resuspended in 2 ml of ice-cold 50 mM $CaCl_2$/15% glycerol and then collected by centrifugation at 3,000 rpm for 10 min at 4ºC. Collected cell were dissolved again, resuspended in 0.05 ml of ice-cold 50 mM $CaCl_2$/15% glycerol and divided equally into two test tubes. 2 µl of the plasmid DNA to be analyzed and the control DNA (vector only) were added in separate tubes and incubated on ice for 30 min. The competent cell mixture was heat shocked at 42ºC for 2 min, then mixed with 0.5 ml of LB medium and incubated at 37ºC for 60 min. The cells were spread on LB plate containing appropriate antibiotics and incubated at 37ºC overnight.

2.7 Measurement of cell wall strength

The tested strains were grown overnight in LB medium containing appropriate antibiotics. Cells were diluted to 1/100 dilution and grown in LB medium at 37 ºC. The samples of 2 h, 5 h and 24 h cultures were diluted to 1/10 with LB or water and the absorbance (OD600) of each dilution was measured. Cell wall strength was presented by the ratio of absorbance of the culture diluted with water ($OD_{600}{}^{water}$) to LB ($OD_{650}{}^{LB}$).

Cell wall strength = $OD_{600}{}^{water}/ OD_{650}{}^{LB}$

2.8 BATCH analysis and β-Galactosidase assays

BACTH assay was detected by the coloring of the colonies on X–gal plate. The two recombinant plasmids encoding the T25-X (or X-T25) and T18-Y (or Y-T18) hybrid proteins were transformed into indicator strain JE8471. The resultant transformants were streaked on the LB medium containing antibiotics and X-gal (40 µg/ml) and incubated at 30 ºC. The blue colonies indicated the positive interaction, while the white colonies means no interaction between both tested proteins (Figure 6).

The efficiencies of complementation were measured by β-Galactosidase assay as described in Miller (1972) with minor modifications. Resultant transformants were once purified and grown on LB plates containing antibiotics for 24 h at 30°C. An appropriate amount

of cells from each transformant were suspended in LB medium for OD600 of about 0.4-0.6 (Kippert, 1995). The 300 µl sample was added into 350 µl of Z buffer containing 0.2% of sarkosyl. The mixture of the sample and Z-buffer was incubated at 30 °C for 30 min before 150 µl of ONPG (O-nitrophenyl galactopyranase) solution was added and incubation was continued until a yellow color developed. The reaction time was measured and the reaction was stopped by adding 375 µl of 1M Na_2CO_3 when sufficient color was observed.

Z-Buffer (200ml)

60mM $Na_2HPO_4.12H_2O$	4.3g
40mM $NaH_2PO_4.2H_2O$	1.24g
10mM KCl	0.15g
1mM $Mg_2SO_4.7H_2O$	0.05g

After autoclave, add 270 µl β-Mercaptoethanol (50mM)

For the lysis of cells, add 0.4g Sodium Lauryl Sarkosyl salt (final= 0.2%)

ONPG

40mg	ONPG
10ml	Z-Buffer (without Sarkosyl)

1M Na_2CO_3

10.5g	Na_2CO_3
100ml	Deionized H_2O

The sample was centrifuged at 3,000 rpm for 5min and the OD_{420} and OD_{550} was measured. The activity was calculated using the formula;

$$\text{Activity (Miller Units)} = \frac{1000 \times (OD_{420} - 1.75 \times OD_{550})}{OD_{600} \times \text{Time (min)} \times \text{Volume (ml)}}$$

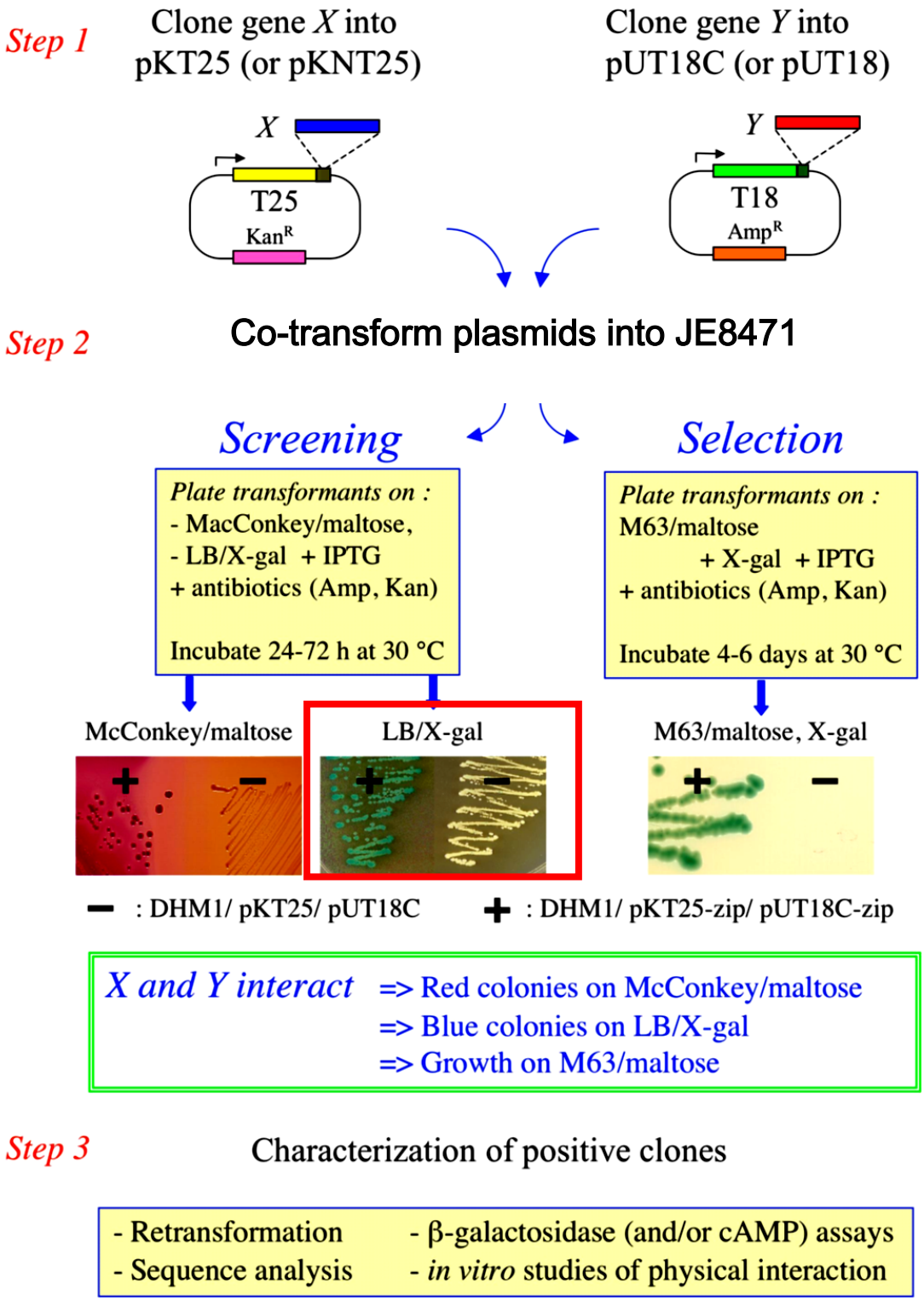

Figure 6: General methodology of analyze protein-protein interaction by BACTH system (www.euromedex.com)

2.9 Integration of fusion genes into chromosome by Lambda InCh

Chromosomal integrations of *araC* P^{ara}*BAD-yciB* were performed via phage λInCh (Figure 7) as described (Boyd *et al*., 2000).

Lysate preparation: A single colony of the strain carrying the *araC* P^{ara}*BAD-yciB* fusion plasmid was grown overnight in LB medium containing 2 mM Mg_2SO_4 and 0.2% maltose with appropriate antibiotics. 0.1 ml of ON culture was mixed with 0.01ml of λInCh (prepared from strain JOE59 (SM551), a lysogen of λInCh for pBR derivatives) and incubated at 30 °C for 15 min. Then, 1 ml LB + MgSO4 (2 mM) was added and mixed for an hour at 30 °C. The mixture was spread on plates containing both 0.04 mg/ml kanamycin and 0.1 mg/ml ampicillin and incubated overnight at 30 °C. Several colonies were purified on the same plate and incubated at 30 °C.

The culture without lambda infection was used as control to make sure only λInCh-containing strains were selected. Single colonies were picked up, grown in 0.5 ml LB at 30 °C for approximately 8h to overnight before spotting on normal LB plate and LB plate containing both ampicillin and kanamycin, and incubated at 42 °C and 30 °C, respectively. The rest of the above LB culture was left on the desk until required. The culture that was temperature sensitive (Tm^S) at 42 °C was selected and 0.2ml portion was inoculated into 5 ml of LB containing ampicillin. Cells were grown with good aeration at 30 °C until OD_{600} was approximately 0.5, heated at 42 °C for 15min to induce the propagation of λ, then immediately transferred to 37 °C and further cultured for approximately 2~3 h. Next, cells were collected at 3,000 rpm for 10 min and suspended with 0.8 ml SM buffer, lysed by adding 50 ml chloroform and then vortexed. The success of λ propagation was ensured by observing the viscosity and the lysate was stored at 4 °C until needed.

Infection of LE392: A *supF* strain, LE392 was grown in LB medium containing 2mM Mg_2SO_4 and 0.2 % maltose ON and 0.05 ml was mixed with 0.05 ml of serial dilutions of lysate described above and then incubated at 30 °C for 15 min. 0.5 ml LB + Mg_2SO_4 (2 mM) was added and incubated for an hour at 30 °C, then a portion of 0.1ml was spread on plates containing ampicillin and incubated at 30 °C overnight. Several colonies were purified on the same plate and incubated at 30 °C overnight. Subsequently, single colonies of each Amp^R clone were picked up, grown in 0.5 ml LB at 30 °C for approximately 8h to overnight and spotted on LB plate and LB plate containing both ampicillin and kanamycin. The LB plate was incubated at 42 °C and the plate containing both ampicillin and kanamycin was incubated at 30 °C overnight. The rest of the above 0.5 ml of LB culture was kept until required. Clones that

showed Tm sensitive, kanamycin sensitive and ampicillin resistance phenotype, should be the lysogen of λInCh recombinant that acquired *araC* P^{ara}*BAD-yciB* fusion and Amp^R from the plasmid. A portion of the corresponding culture was inoculated into 1ml LB and cells were grown at 30 °C until the OD_{600} was approximately 0.5, heated at 42 °C for 15min and incubated at 37 °C for approximately 3 h to observe for complete lysis. Two drops of chloroform was added and shaking continued at 37 °C for another 15min. The supernatant was collected at 3,000 rpm for 5min and transferred into a new tube and stored as pure lysate of λInCh recombinant for *araC* P^{ara}*BAD-yciB* fusion.

Transfer of lambda integrated *araC* P^{ara}*BAD-yciB* fusion into the WT strain: The WT strain was grown overnight in LB medium containing 2mM Mg_2SO_4 and 0.2% maltose. A 0.05ml portion of overnight culture was mixed with 0.05ml aliquots of 1/100 dilution of pure lysate and then incubated at 30 °C for 15min. 0.5ml LB + $MgSO_4$ (2mM) was added and mixed for an hour at 30 °C before streaking 0.1ml on plates containing ampicillin. The plates were incubated at 30 °C overnight. Colonies were purified on the same plate and single colonies were picked up as above to inoculate in 0.5ml LB medium. Cells were grown at 30 °C streaked on LB plate containing ampicillin and incubated at 42 °C overnight. Colonies that appeared (Tm^R) should have lost the parts of lambda required for propagation and were purified once more at 42 °C. Resultant clones containing the *araC* P^{ara}*BAD-yciB* fusion on the chromosome were examined for the sensitivity to antibiotics and used for the growth assay.

2.10 Protein extraction, purification and binding.

Extraction: Cells were cultured in 2 ml LB medium overnight at 37 °C with the appropriate antibiotics. Cells were grown in 30 ml LB medium with appropriate antibiotics at 37°C until OD600 reached to ~ 0.5, then induced with 0.2% arabinose (final concentration) or 0.5 mM IPTG depends on the promoter. The cells were collected after 1 h induction and centrifuged at 3,000 rpm for 10 min. Then, the cells were lysed and proteins extracted by adding Bugbuster Protein Extraction Reagent (Novagen) (5 ml/g cells) incubating for 20 min at room temperature with gentle rotation. Centrifugation was carried out at 15,000 rpm for 10 min at 4°C and transferred the supernatant to fresh tube as cell lysate.

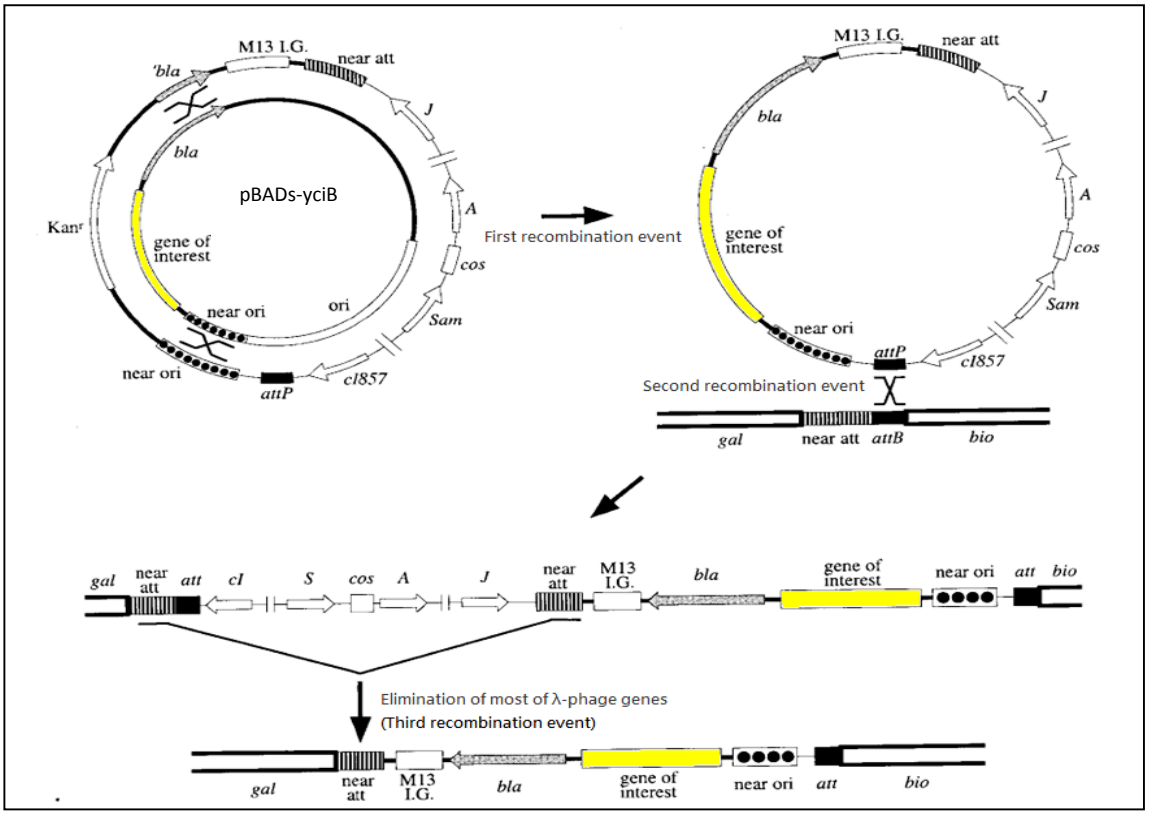

Figure 7: Integration of *araC P*^{ara}*BAD-yciB* fusion into chromosome.

There are three major steps involved in the integration of *araC P*^{ara}*BAD-yciB* fusion into chromosome. At the upper left, the plasmid and the phage are shown as concentric circles with the phage outside. In the first step, recombination at both the 358-bp *bla* region and the 409-bp near ori region results in transfer of the promoter gene expression and a functional bla (Amp^r) gene to the phage replacing the Kan^r gene. In the second step, a lysogen is formed by site-specific recombination at the *att* site, conferring ampicillin resistance and temperature sensitivity. The orientation at the *att* site is indicated relative to the flanking markers *gal* and *bio*. In the third step, recombination in the 800-bp direct-repeat region, near-att, removes most of the phage DNA conferring temperatures independence. The att region in the stabilized strain is shown at the bottom (Boyd et al., 2009).

Purification: The extracted S-tagged fusion proteins were purified using COSMOGEL His Accept. Proteins in a lysate were trapped on gel using 1 ml Buffer I and eluted with 400 µl of Elution Buffer. The buffer of purified proteins was changed to PBS buffer by centrifugation through a 10 kDa cut off UltraFree MC (Amicon). Meanwhile, T18-ZipA was concentrated using Microcon YM-30 and centrifugation at 13,000 rpm for 12 min.

Binding: A protein that was purified and other in crude cell extract were mixed and incubated for 30 min at RT. The mixtures was applied to 1 ml COSMOGEL His Accept equilibrated with Buffer I and rotated gently for 20 min. The bound proteins were eluted with 100 µl Elution Buffer three times and samples were analysed on a 12.5% SDS-PAGE gel followed by Western Blotting.

Solutions:

Buffer I

1 M HEPES (pH 8.0)	10 ml
NaCl	2.58 g

Adjusted to 100 ml with deionized H_2O

Elution Buffer

1 M HEPES (pH 8.0)	10 ml
NaCl	2.58 g
Imidazole	3.4 g

Adjusted to 100 ml with deionized H_2O

Wash Buffer

0.1 M MES (pH 5.0)	20 ml
NaCl	0.57 g

Adjusted to 100 ml with deionized H_2O

*All solutions were autoclaved before use

2.11 SDS-PAGE

The protein samples were mixed with an equal volume of 2×SDS loading buffer. The mixture was heated and then loaded on to a 12.5% SDS-PAGE. The SDS-PAGE gel were prepared with the solution as listed below:

Solutions:

2×SDS loading buffer

0.25 M Tris/HCl (PH 6.8)	25 ml
β-mercaptoethanol	5 ml
SDS	2 g
Sucrose	5 g
Bromophenol blue	2 mg
Make up to 50ml with H_2O	

12.5% SDS-Gel:

Separating Gel		Stacking Gel	
Solution A	3 ml	Solution A	0.35 ml
Solution B	1.8 ml	Solution C	0.6 ml
TEMED	7.5 µl	TEMED	2.5 µl
10% APS	75 µl	10% APS	25 µl
H_2O	2.4 ml	H_2O	1.45 ml

Solution A (30% Acrylamide):

Acrylamide	29.2 g
N,N'-methylenebisacrylamide	0.8 g
Make up to 100 ml with water.	

Solution B (1.5M Tris-HCl buffer, pH 8.8)

Tris	18.2 g
SDS	0.4 g
HCl	2 ml
Make up to 10oml with water	

Solution C (0.5M Tris-HCl buffer, pH 6.8):

Tris	6.1 g
SDS	0.4 g
HCl	4.2 ml

Make up to 100 ml with water.

SDS running buffer (pH ~8.5):

Glycine	57.6 g
Tris	12 g
SDS	4 g

Make up to 4 L with water.

Electrophoresis was performed at room temperature under the constant current of 25 mA using Mini-gel electrophoresis apparatus (ATTO, Japan).

2.12 Western blotting analysis

After separation by SDS-PAGE, proteins were transferred to a PVDF membrane by semi-dry blotter PoweredBLOT-ONE (Atto) for 10 min according to manufacturer's protocol. This rapid mode was selected with the usage of EzFast Blot reagent. The filter papers and PVDF membrane were pretreated with 1x Ez-Fast Blot reagent (Atto) for 10 min before blotting. After that, the blotted membrane was soaked into Blocking One Solution (Nacalai) for 1 h and then washed with TBST for 1 min. The blocked membrane was soaked in TBST-BSA (Wako) (0.3 %) buffer containing properly diluted primary antibody and incubated for 30 minutes at room temperature. Antibody anti-CyaA (3D1) (Santa cruz biotechnology) was used at the concentration of 1~2 µg/ml.

The membrane was washed three times with TBST buffer, and soaked into TBST-BSA (0.3%) buffer containing labeled secondary antibody and incubated for 30 minutes at room temperature. Anti-mouse IgG HRP conjugate (Promega) was used at 5,000-fold dilution. The membrane was washed three times with TBST buffer and proteins were detected by the method appropriate to the secondary antibody. To detect proteins with horseradish peroxidase (HRP) conjugated secondary antibody, Chemi-Lumi One L reagent (Nacalai) was used to give chemiluminescence signal. The washed membrane was completely covered with mixture of Solution A and B of Chemi-Lumi One L reagent for 1 min and the solution removed with paper

towel. The bands of the target proteins were visualized by FujiFilm LAS-1000plus Luminescent Image Analyzer.

For the detection of S-tagged proteins, the blotted membrane was soaked into TBST solution containing S-protein HRP conjugate (Novagen) (1:5000 dilution) for 30 min. The membrane was washed with TBST four times and the S-tagged proteins were detected by reaction with Chemi-Lumi One L reagent.

TBST

1 M Tris-Cl (pH8)	5ml
NaCl	4.5g
H_2O	to 500ml
Add Tween 20	0.5ml

2.13 Microscopy

Subcellular localization of GFP-fusion protein and DIC image of cell was examined microscopically by Olympus Fluoview FV1000-D system using a 100 x oil immersion (N.A. 1.4) objective on BX61WI microscope. The *E. coli* strains to be examined were grown overnight in LB broth containing appropriate antibiotics. The cultures were diluted in LB medium containing appropriate antibiotics and IPTG (25 μM/50 μM/500 μM) or L-arabinose (0.1% - 0.2%) when required and grown as indicated. Cells were fixed in the growth medium by adding one volume of 4% paraformaldehyde-phosphate buffer solution (Nacalai) and incubating for 10 min at room temperature. Fixed cells were collected by centrifugation, washed three times with PBS (10 mM Na_3PO_4 [pH 7.4], 150 mM NaCl, 15 mM KCl). Two miro litres of cell suspension was deposited on the glass slide.

2.13.1 Immunofluorescence microscopy

For detecting proteins expressed from a chromosome integrated gene, immuno-staining with Alexa488 was performed due to the weak fluorescence signal. The cells were grown and fixed as described above. Then, the fixed cells were permeabilized with 0.1% TritonX in PBS for 10 min and washed two times with PBS. Cells were dissolved in 100 μl of Blocking One solution, and incubated for 30 min. The samples were washed two times with PBS. After that, the samples were incubated for 30 min at RT with 100 μl of anti-GFP in 3% TBST/BSA

(1:5000 dilution) and washed three times with PBS. Next, the samples were incubated for 1 h in 100 µl of donkey anti-rabbit antibody conjugated with Alexa Fluor 488 (Biotium) (1:5000 dilution with 3% TBST/BSA) and washed again.

Strain KR1431 (λP_{araBAD}-*yciB*) was stained using S-protein conjugated with FITC. The permeabilized cells were incubated with S-protein FITC (1:5000 dilution) in PBS for 1 h at room temperature in the dark. The sample was washed three times with PBS and re-suspended in 50 µl PBS.

The stained culture was deposited on 0.1% poly-L-lysine coated slide and cured with ProLong® Diamond Antifade Mountant with DAPI (Life Technologies) or SlowFade Diamond Antifade Mountant without DAPI (Life Technologies) as described in procedure provided by manufacturer. The slide was then incubated for 24 h at RT in the dark and observed.

Solution:

PBS Buffer:

PBS tablet (Takara bio, Japan)	1 tablet
Deionized H_2O	100ml
measure pH	

3. RESULTS

3.1 Characterization of Δ*yciB* mutant and its product YciB

3.1.1 The sensitivity of the Δ*yciB* mutant to osmotic stresses

The *yciB* gene was identified as a gene that affects biofilm formation upon its deletion. It was also found genetically to interact with *rodZ* (Niba *et al.*, 2007). The deletion mutant of *yciB* (Δ*yciB*) grows more slowly compared to wild type but shows neither temperature sensitivity nor morphological abnormality. However, it is conceivable that the Δ*yciB* mutant has some abnormality in the membrane integrity because membrane properties would affect the biofilm formation. To investigate this possibility and the function of *yciB*, we first examined the sensitivity of the mutant to osmotic stresses. As shown in Figure 8, the growth of KR1411 (Δ*yciB*) was significantly delayed under the low osmotic condition (0% NaCl). On the other hand, the mutant grew slightly better in the high osmotic condition (1% NaCl) compared to the standard LB medium, which was not the case of the wild type strain KR0401. This suggested that the cell wall of the Δ*yciB* mutant had a defect rendering it sensitive to the turgor pressure. Resistance of the mutant to the osmotic shock was also reduced significantly in the logarithmic growth phase (Figure 9).

These phenotypes were partially recovered by plasmid pBADs-*yciB* carrying an L-arabinose inducible *yciB* gene (P_{araBAD}-*yciB*). However, the growth of KR1411 (Δ*yciB*) carrying the plasmid pBADs-*yciB* was severely hindered in the presence of 0.2% L-arabinose (Figure 10). Growth inhibition by the induction of *yciB* was also observed in wild type cells but the effect seemed considerably greater in the Δ*yciB* mutant. It was reported that most of membrane proteins somehow inhibit the cell growth when over produced even though they are not toxic themselves, because overproduced membrane proteins would inhibit the transport of other membrane proteins and proper localization (Wagner *et al*., 2007). However, this reason cannot explain the severer phenotype by overexpression in the Δ*yciB* mutant.

3.1.2 YciB affects the cell length.

Because our previous investigation of Δ*yciB* mutant and the reports about its homolog in *S. flexneri* described above indicated that *yciB* might participate in cell elongation and/or cell division, we observed microscopically cell morphology and measured the cell length of Δ*yciB* mutant as well as of the cell that is overproducing YciB. The results obtained showed that Δ*yciB* mutant is 40% shorter than wild type (Figure 11). Because the growth rate of

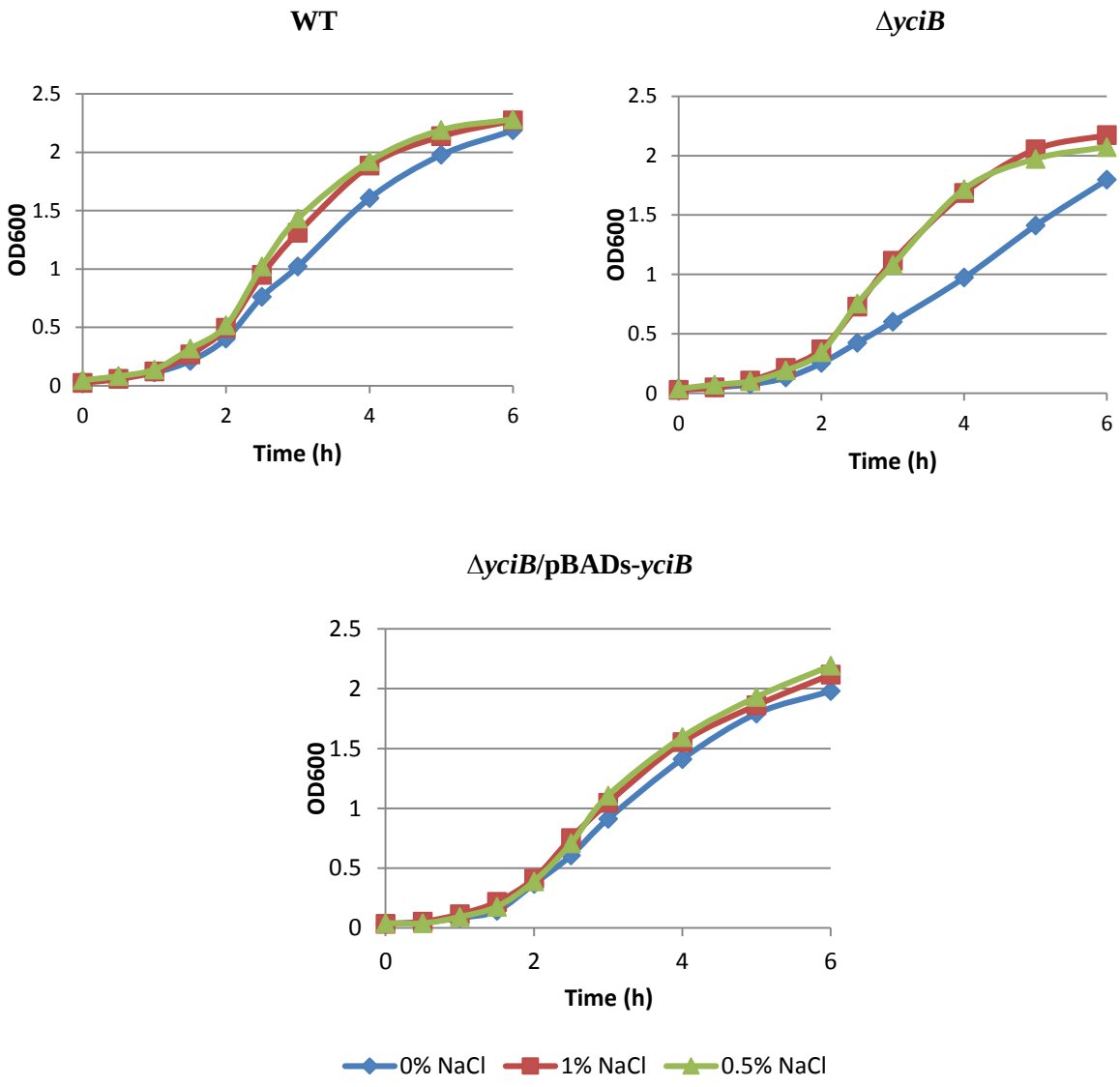

Figure 8: Effects of Δ*yciB* mutations on cell growth under different osmolarity condition.

KR0401 (WT), KR1411 (*ΔyciB*) and KR1411 carrying pBADs-*yciB* (*ΔyciB/* pBADs-*yciB*) were grown in LB medium (0.5% NaCl) (green), LB containing 1% NaCl (red) and salt free LB (0% NaCl)(blue) at 37 ºC and OD600 were measured at indicated time intervals.

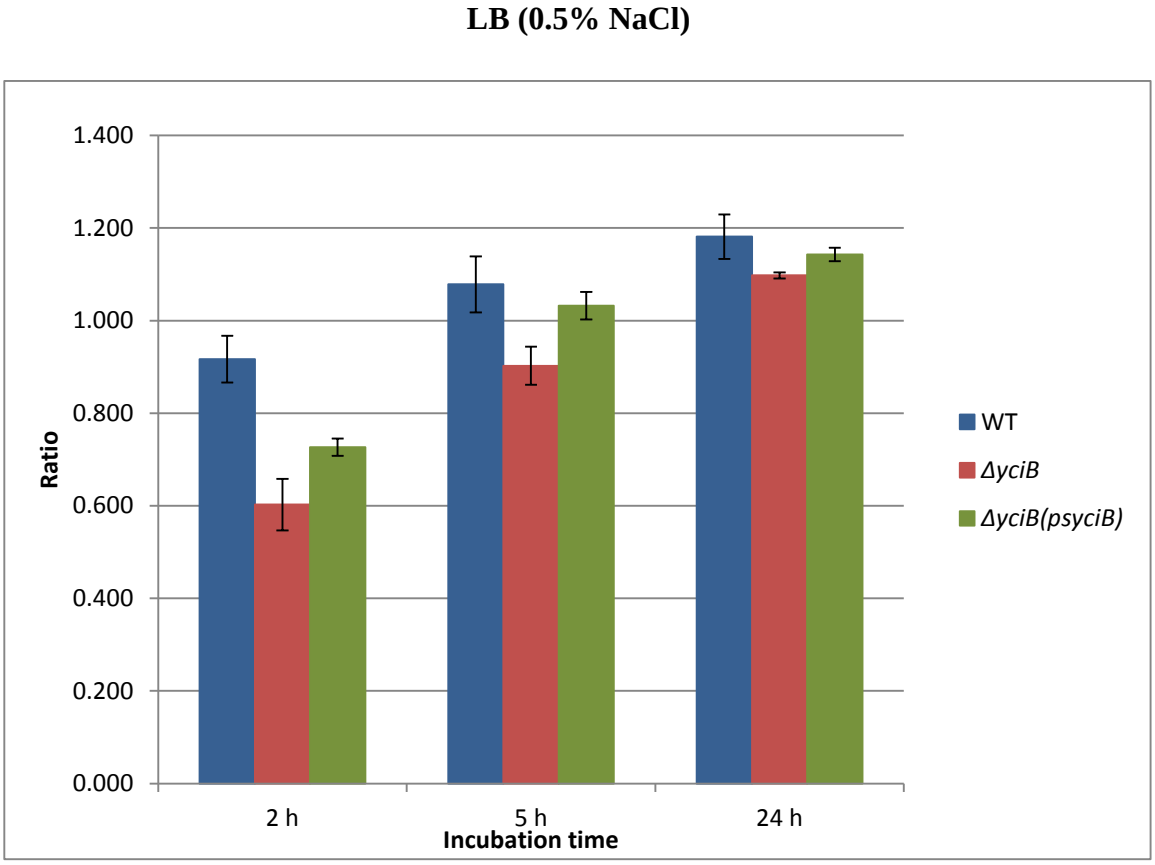

Figure 9: Sensitivity of Δ*yciB* to the osmotic shock.

Aliquots of the cell cultures in LB medium of KR0401 (blue), KR1411 (red) and KR1411 carrying plasmid pBADs-*yciB* (green) were taken at mid-(2 hours), late-logarithmic (5 hours) or stationary phase (24 hours) and diluted (10 fold) either in LB medium or water. The ratio of measured OD600 of water to LB dilution were presented as cell wall strength. Averages of three independent experiments are shown with standard deviation.

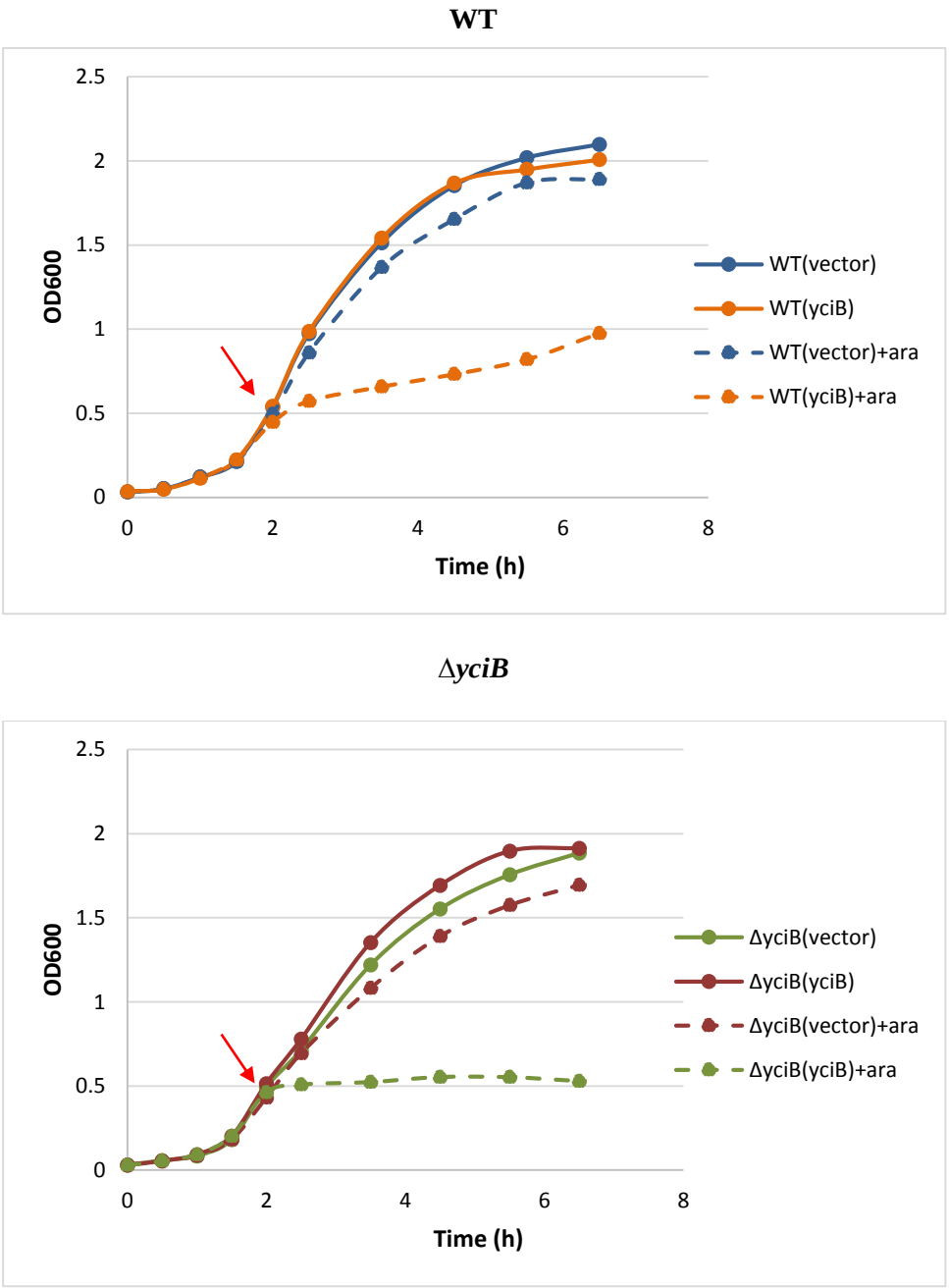

Figure 10: Effect of the YciB overproduction to the cell growth.

KR0401 (WT) (upper) and KR1411 (*ΔyciB*) (bottom) carrying pBADs or pBADs-*yciB* were cultured at 37 ºC in LB medium. At indicated time (arrow), the cultures were divided and 0.2% L-arabinose were added to one portion. Aliquot of each culture were taken and OD600 were measured at indicated time intervals. Solid (___) and dotted (----) lines indicate the culture without and with arabinose, respectively.

Δ*yciB* mutant is reduced (Figure 8), we consider that this shorter cell length is not due to the accelerated cell division as in the case of *opgH* mutant (Hill *et al*., 2013), but due to a defect in the peptidoglycan synthesis. On the other hand, the induction of *yciB* on plasmid pBADs-*yciB* with 0.2% L-arabinose for one hour increased the cell length about two fold both in wild type and the mutant (Figure 12). The analysis of longer cells stained with DAPI seems to indicate that the elongation is not due to a failure of the cell septation as in the case of *zipA* overproduction (Hale and de Boer, 1997), but rather, the lateral cell envelope of each cell was elongated. Some cells also appear to have abnormality in chromosome segregation. Further induction (over two hours) seemed to give a severe damage on the cell envelope. The lysis of cells appeared to start and eventually the growth was inhibited (Figure 11). The abnormality of cells was more prominent in the Δ*yciB* mutant. Occasionally filamentous cells or those significantly greater both in length and width were also observed. This might indicate that not only the presence of YciB in the cell but also in a proper ratio to other proteins involved in the synthesis of cell envelope is important, which will impose a larger adjustment on the Δ*yciB* mutant cell compared to the wild type at a sudden increase of YciB protein. Cell lysis and the occurrence of filamentous or gigantic cells by overproduction of YciB might have been brought about by a defective septum formation, because the cell surface often appeared abnormal at the mid-cell and the cell-pole that could be the previous septum site (Figure 12). These observations together with the report of *ispA*, the *S. flexneri* homolog of *yciB*, being involved in cell division (Mac Síomóin *et al.*, 1996) seems to indicate that *E. coli yciB* also participates in the cell division process.

3.1.3 YciB interacts with cell division and cell elongation proteins by BACTH analysis

In order to investigate the above possibility, I next examined the interaction of YciB with divisome components by a bacterial two-hybrid (BACTH) system (Karimova *et al.*, 1998). This system is based on reconstitution of adenylate cyclase activity and the expression of *lacZ* reporter gene when the T18 and T25 domains of *Bordetella pertussis* CyaA are brought close together through interactions between fusion partners. Here, the T18 and T25 fragments must be located in the cytoplasm since the reaction was occurred in the cytoplasm. Therefore, CyaA domains are required to be appended at the cytoplasmic domain of each membrane protein. Because YciB contains five trans-membrane regions and its N-terminus is localized in the periplasm (Uniprot, 2014; Li, 2012), T18 fragment of CyaA was C-terminally

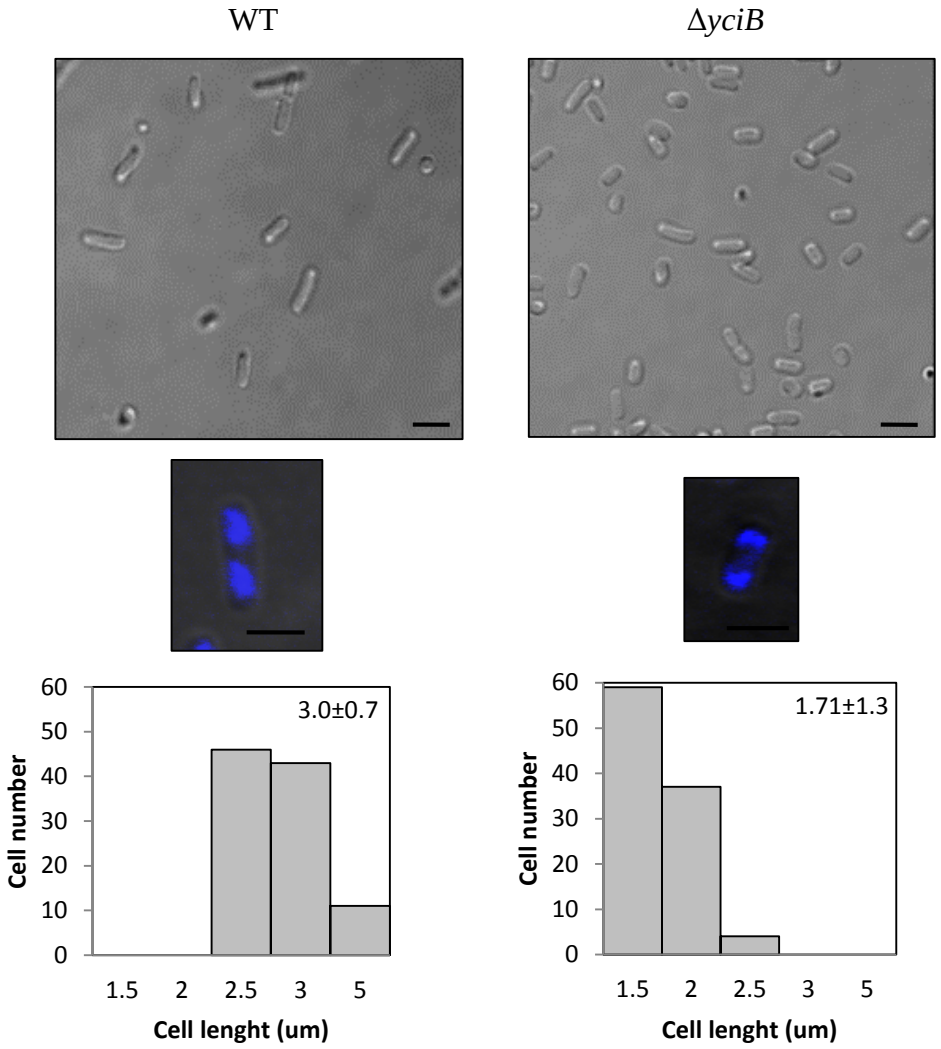

Figure 11: Cell morphology and distribution of cell length in the absence of YciB.

Aliquots of the cell cultures in LB medium of KR0401 (WT) and KR1411 (*ΔyciB*) were taken at ~1.0 of OD600 and fixed with 4% PFA. The samples were observed with or without DAPI staining by fluorescence microscope. The length of the 100 cells were measured and shown in the histograph with the average and standard deviation. Scale bar = 2 µm.

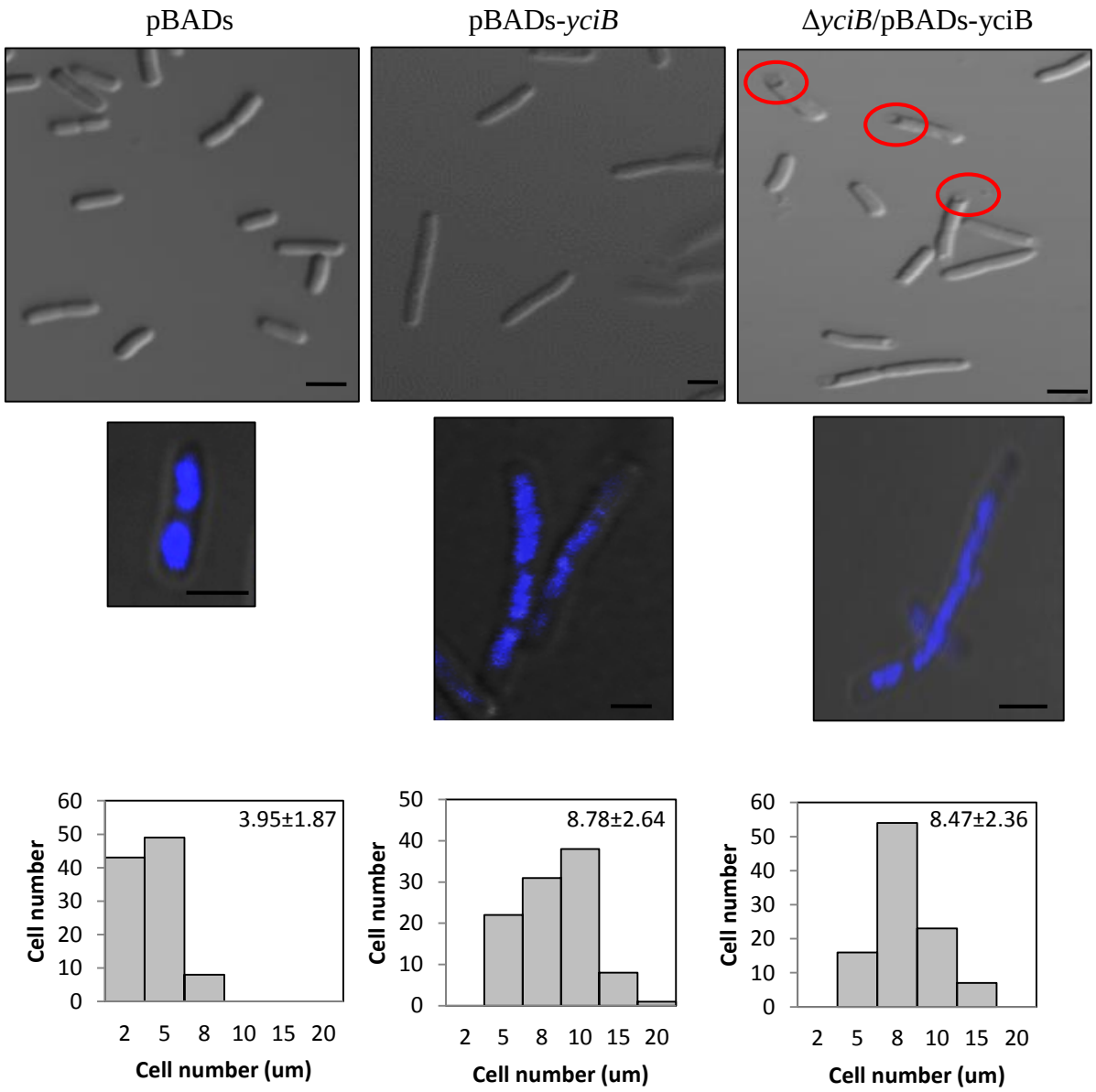

Figure 12: Cell morphology and distribution of cell length in overexpression of *yciB*.

Aliquots of the cell cultures in LB medium of KR0401 (WT) and KR1411 (*ΔyciB*) carrying plasmid only and pBADs-*yciB* were taken after 1 hour induction by 0.2% L-arabinose and fixed with 4% PFA. The samples were observed with or without DAPI staining by fluorescence microscope. The length of the 100 cells were measured. Histograms show the distribution of cell length with the average and standard deviation of each strain. Scale bar = 2 µm.

fused to YciB on the plasmid pUT18, and T25 was appended to the cytoplasmic region of each cell division protein.

I also investigated which region of YciB is required for the interaction using deletion mutants of *yciB*. YciB is predicted to encode 179 amino acid residues containing five transmembrane domains. As shown in Figure 13(a), I constructed truncated versions of YciB-T18 fusion. The results obtained with these constructs revealed that YciB interacts with most of divisome proteins examined, but not with FtsZ septal ring protein (Figure 14(b)). In addition, the activity of ß-galactosidase by protein interaction was higher with the C-terminally truncated YciB fusion proteins, YciB-170 (43kD) and YciB-118 (39kD) compared to the full-length YciB-FL (45kD). The reason for this seems to be the lowered expression of *yciB* gene or instability of YciB-FL (Figure 13(b)), probably due to the toxicity of overproduced YciB as indicated above. However, the YciB48 (amino acid residues 1-48) showed a low activity of β-galactosidase indicating that the middle cytoplasmic and the second TM regions from the C-terminus of YciB structure were required for protein-protein interaction.

Similarly, I examined the interaction of YciB with proteins of elongation complex (Figure 14(a)) YciB interacted clearly with MreC, MreD, RodA and RodZ. MurG, the N-acetylglucosaminyl transferase responsible for the final intracellular step of peptidoglycan subunit assembly, also showed a strong interaction. On the other hand, MreB interacted only weakly. However, YciB showed no interaction with MalF and MalG of maltose transport complex, which demonstrates that YciB does not merely interact with inner-membrane proteins.

3.1.4 YciB is not focused at the septum site and localized along the membrane through the whole cell.

Because YciB showed interactions with various proteins of divisome, I examined whether YciB is also localized at the septum-forming site using an ASKA clone, pCA24N-*yciB,* expressing YciB-GFP fusion protein (Kitagawa *et al.,* 2005). Fluorescence microscopy revealed that the fusion protein did not accumulate at division sites as observed with most of divisome components. It appeared to be distributed in the inner membrane through the whole cell (Figure 15). Next, I observed the localization of YciB-GFP with strain KR1436 (λP_{araBAD}-*yciB-GFP*) that expresses YciB-GFP from the chromosome integrated gene and

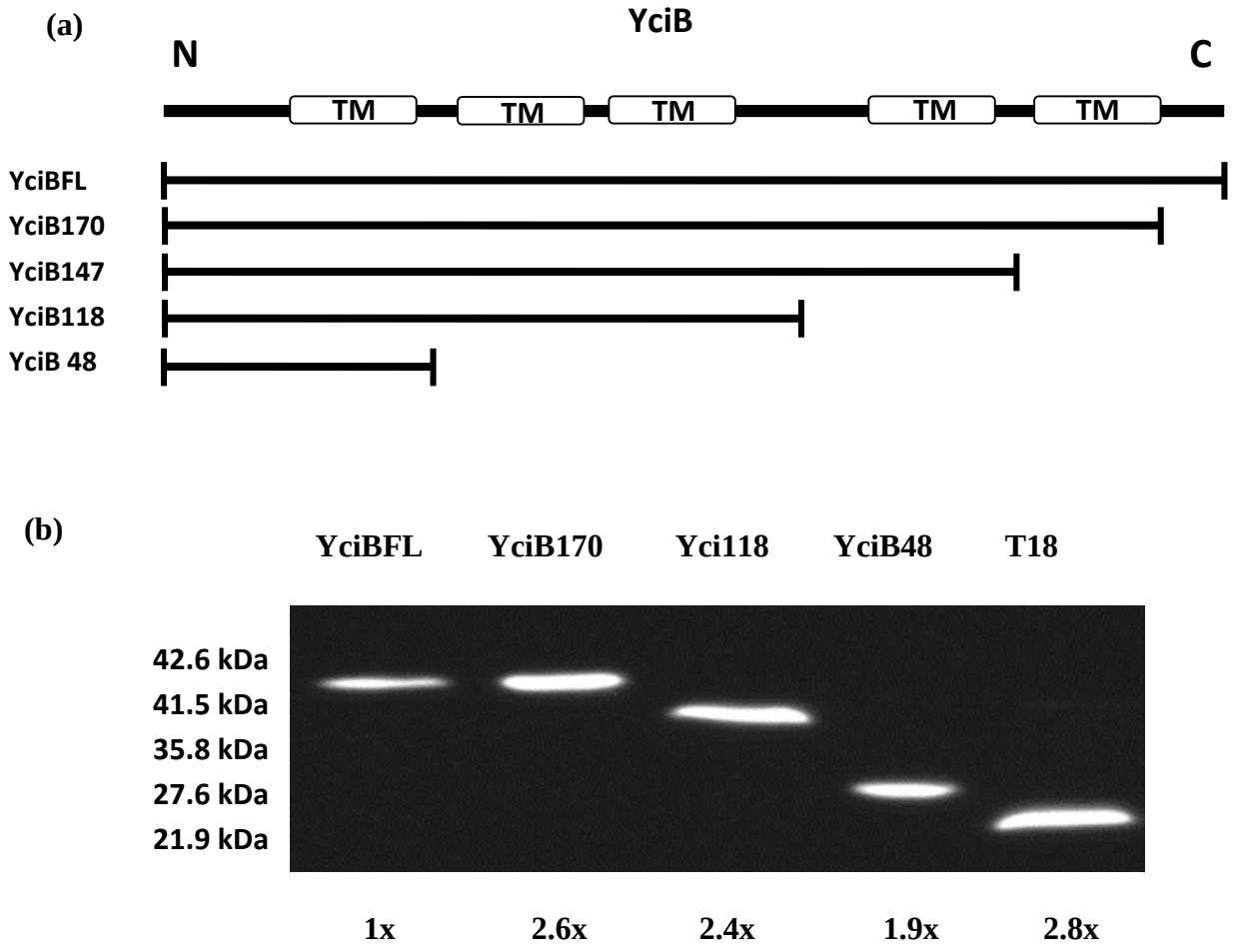

Figure 13:(a) The physical map of the yciB gene constructed in this study. (b) Expression level of T18-YciBFL and its truncated variants.

Cells expressing the indicated proteins were cultured in LB medium containing ampicilin at 37 ^{o}C until OD600 reached ~1.0. Proteins were extracted by Bug Buster reagent and separated on SDS-PAGE. The proteins were transferred to PVDF membrane and probed with anti-CyaA (T18) antibody. The chemiluminescent signal were detected by LAS1000 imaging system. The protein expression level were quantified by LAS Image Gauge imaging system.

(a)

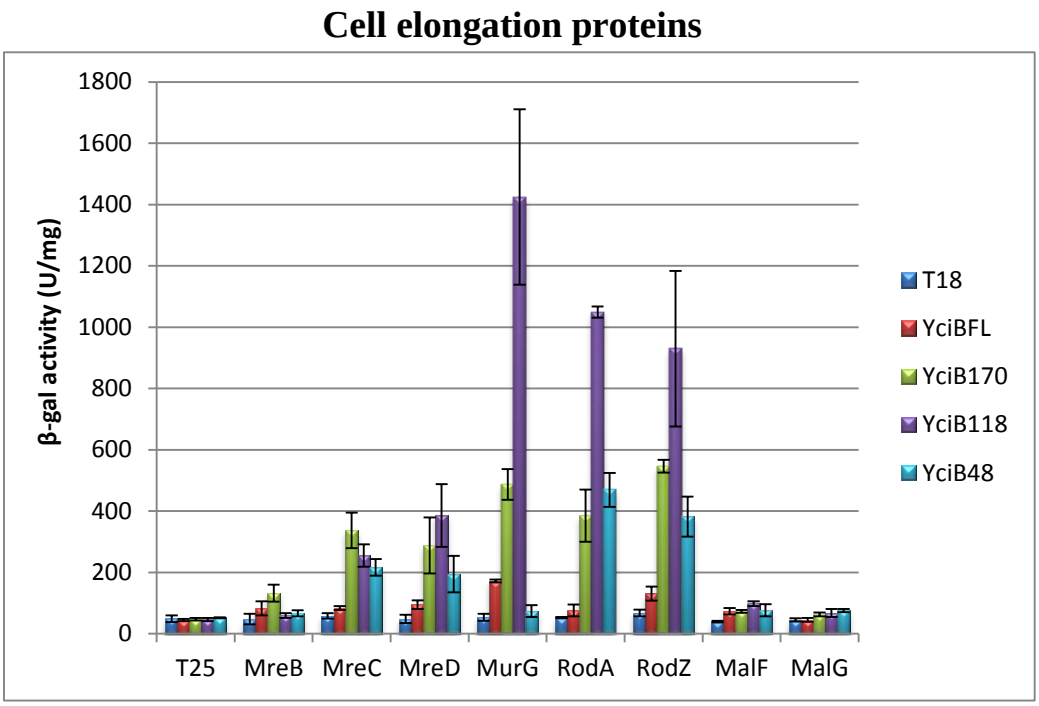

(b)

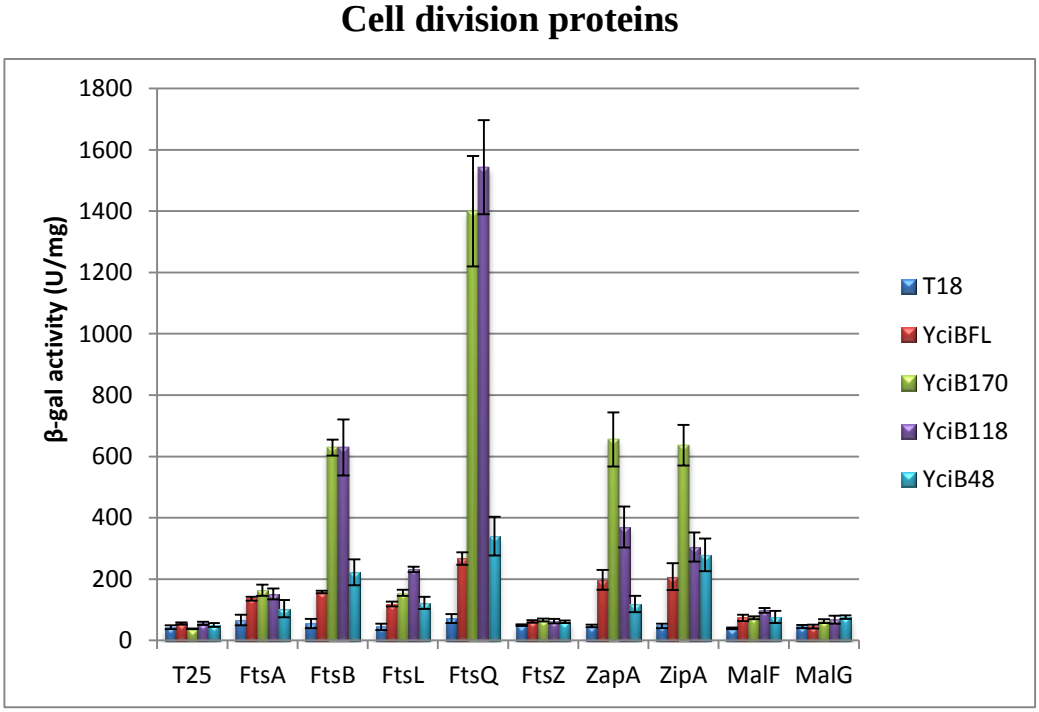

Figure 14: β-galactosidase assays of protein interaction between YciB (a) cell elongation proteins or (b) cell division proteins.

Transformants expressing tested proteins were resuspended in LB medium at about OD600 0.4-0.6 and β-galactosidase assays were carried as described in Materials and Methods. Average and standard deviation were calculated from the measured activities of three independent analysis.

avoids the overproduction of YciB. For this chromosome integrated YciB-GFP, I used the technique of immunofluorescence microscopy with anti-GFP antibody and anti-rabbit conjugated with Alexa488, because the fluorescence signal of GFP was too weak to detect directly. Furthermore, in order to exclude the possible effect of GFP-tag, I also observed the localization of YciB without GFP-tag using KR1431 (λP_{araBAD}-*yciB*) strain and stained with S-protein conjugated with FITC. As shown in Figure 13, YciB-GFP was observed throughout the cell in both strains, and the image of KR1431 (λP_{araBAD}-*yciB*) strain shows more clearly that YciB is localized in the membrane and not in the cytoplasm as predicted and shown by different examination (Li, *et al*., 2012). This localization of YciB may indicate the role of YciB in peptidoglycan elongation and maintaining the membrane integrity.

3.2 Involvement of YciB in cell elongation

The above results obtained indicated that YciB might be involved in both cell division and cell elongation. Therefore, next I tried to examine the effect of Δ*yciB* mutation in phenotype related to the cell elongation process.

3.2.1 Δ*yciB* mutant exhibits sensitivity to A22

The short cell of Δ*yciB* mutant seems to indicate that YciB somehow participates in the lateral PG synthesis in cell elongation. Therefore, I next examined the sensitivity of Δ*yciB* mutant to A22, which is an inhibitor of the assembly of MreB (Iwai *et al*., 2002). MreB is an *E. coli* actin cytoskeleton and one of the rod-shape determining proteins (Jones *et al*., 2001). The growth of KR0401 (WT) was inhibited by more than 1.5 μg/ml of A22. On the other hand, KR1411 (Δ*yciB*) could not grow in the presence of 1 μg/ml of A22 (Figure 16). This seems to indicate that the Δ*yciB* mutant cell requires a rigid MreB cytoskeleton to maintain the integrity of cell envelope.

Next I examined the complementation of A22 sensitivity by the cloned yciB gene. As shown in Figure 17, only a truncated version of YciB, YciB170, showed a weak complementation if expressed form the arabinose promoter on the multi-copy plasmid pBADs. However, if this construct (P_{araBAD}-*yciB*) was integrated into the chromosome, the full length YciB showed a higher complementation. These results might indicate that not only the presence of YciB but a well regulated expression and a proper molecular ratio with the other proteins in the cell are important for normal cell growth.

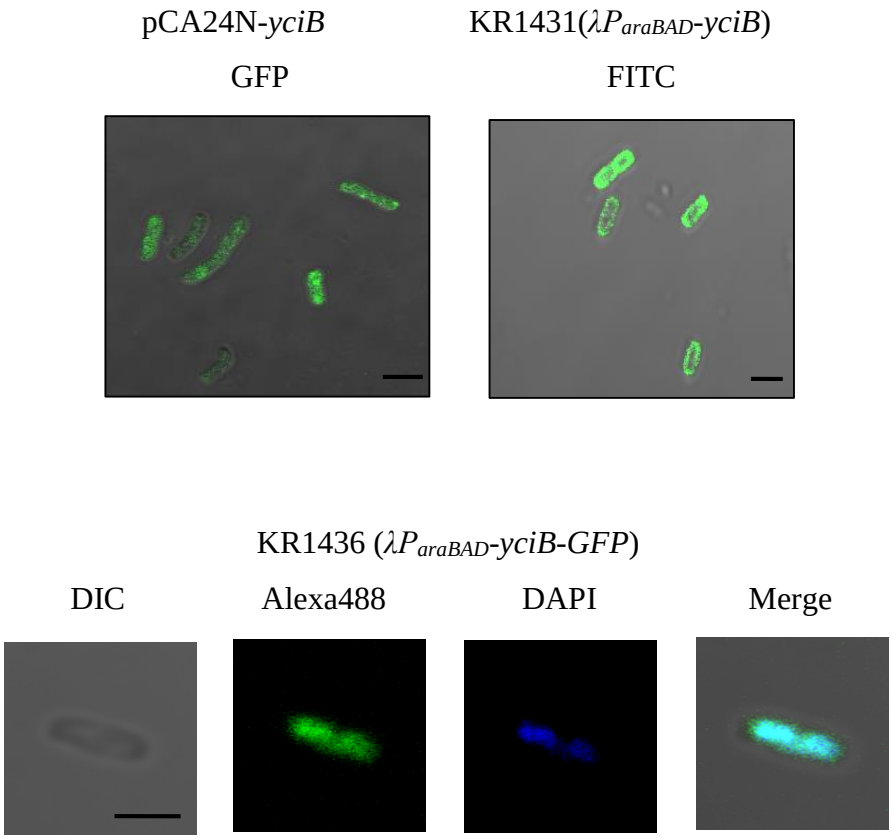

Figure 15: YciB is localized throughout the cell.

Cells expressing YciB-GFP from pCA24N and cells of KR1436 (λP_{araBAD}-*yciB-GFP*) were cultured in LB medium at 37 ºC and induced with 0.5 mM IPTG or 0.2% L-arabinose. The samples were taken at ~0.5 of OD600 and fixed with 4% PFA and observed by fluorescence microscope. YciB-GFP expressed from KR1436 (λP_{araBAD}-*yciB-GFP*) was immunofluorescence stained using anti-GFP and anti-rabbit conjugated with Alexa488. KR1431 (λP_{araBAD}-*yciB*) was cultured in LB medium at 37 ºC and induced with 0.1% L-arabinose. The fixed cells were stained with S-protein conjugated with FITC. The samples were observed by fluorescence microscope. KR1436 (λP_{araBAD}-*yciB-GFP*) sample was also DAPI stained using ProLong Diamond Antifade Mountant with DAPI. The rests were treated with SlowFade Diamond Antifade Mountant without DAPI. Scale bar = 2 µm.

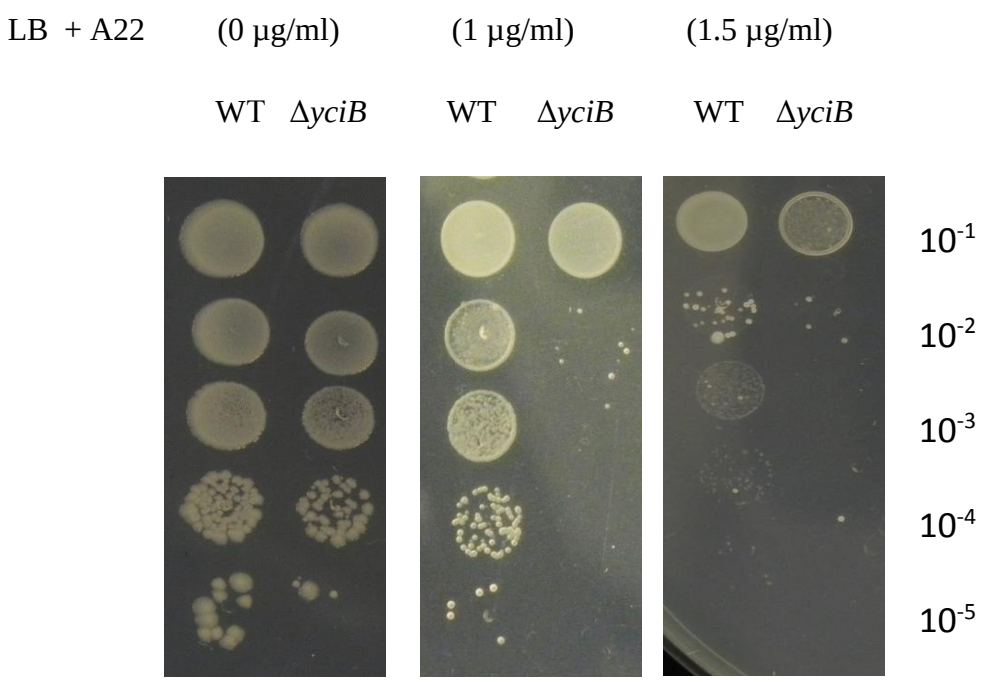

Figure 16: Sensitivity of Δ*yciB* mutant to A22.

KR0401 and KR1411 were cultured at 37 ºC in LB medium until ~OD 0.5 and diluted serially (10^{-1}, 10^{-2}, 10^{-3}, 10^{-4} and 10^{-5}) in LB medium. Five micro litre of each diluent was spotted on LB agar plate containing indicated concentration of A22.

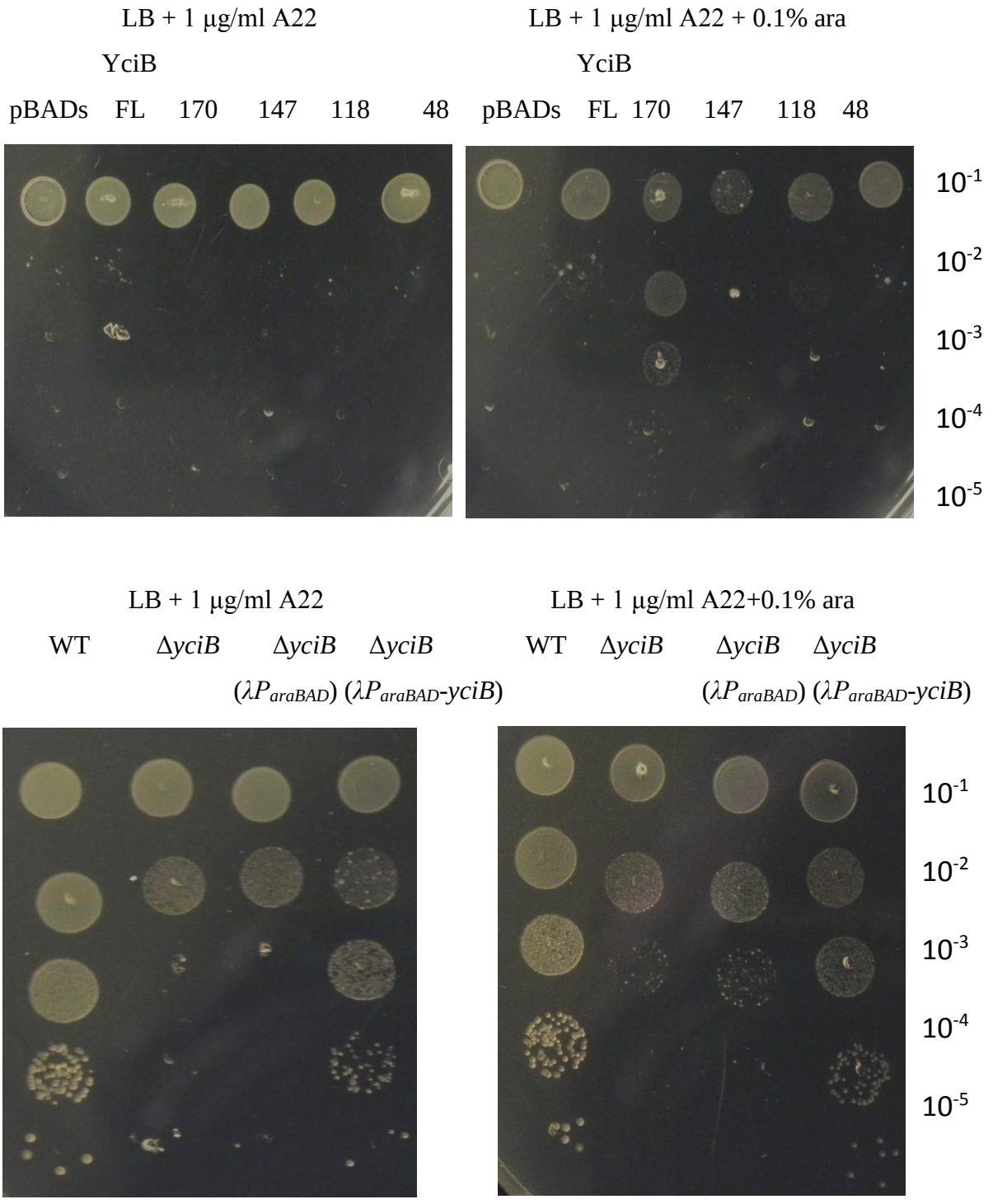

Figure 17: Complementation of *yciB* in Δ*yciB* mutant on A22.

KR0401(WT), KR1411(*ΔyciB*), KR1435 (λP_{araBAD} *ΔyciB*), KR1432 (λP_{araBAD}-*yciB ΔyciB*) and KR1411 carrying pBADS-*yciB* and its truncated variants were cultured at 37 ºC in LB medium until ~OD 0.5 and diluted (10^{-1}, 10^{-2}, 10^{-3}, 10^{-4} and 10^{-5}) in LB medium. Five micro litre was spotted on LB agar plate containing A22 (1 µg/ml) with or without 0.1 % L-arabinose.

3.2.2 Deletion of *yciB* is synthetically lethal in the Δ*rodZ* mutant

Our previous analysis suggested that the deletion of both *yciB* and *rodZ* genes causes synthetic lethality because we were unable to introduce the Δ*yciB::*Kan^R mutation into a Δ*rodZ* strain by P1 transduction (Niba *et al.*, 2007). RodZ is an important protein in maintaining the rod-type cell morphology (Alyahya *et al*., 2009) and probably plays a role in lateral peptidoglycan synthesis (Niba *et al*., 2010). I further examined this phenotype by constructing strains that harbor the Δ*rodZ* Δ*yciB* double deletion mutation and an inducible *yciB* gene integrated in the chromosome, and monitoring the cell growth under *yciB*-induced or repressed conditions. As shown in Figure 18, the growth of KR1434 (Δ*yciB,* Δ*rodZ, P_{ara}-yciB*) was inhibited by the addition of 0.2% glucose that repressed the expression of the *yciB* gene placed under the control of arabinose promoter, whereas this strain could grow in LB medium with and without 0.2% L-arabinose. However, the growth rate was slightly decreased in the presence of 0.2% L-arabinose. Reduced growth by induction of *yciB* was also observed in KR1431 (wild type) and KR1433 (Δ*rodZ*) mutant. These results indicated that *yciB* is essential in the Δ*rodZ* mutant but its over-expression, even of a single gene, decreased the growth rate.

3.2.3 Overexpression of YciB suppressed the sphere shape of Δ*rodZ* mutant cell

Next, in order to investigate more closely the relation between RodZ and YciB, I observed the cell morphology of these strains under repressed and induced conditions. In the presence of L-arabinose most of KR1433 and KR1434 cells were elongated and not spherical, although their shapes were irregular or tapered at the pole instead of the normal rod type (Figure 19). While in the absence of L-arabinose, they showed the same spherical shape as the Δ*rodZ* mutant. Excess YciB might have caused the elongation of Δ*rodZ* mutant by delaying the progress of cell division cycle and hence giving the mutant more time to elongate laterally. The induction of *yciB* in the wild type (KR1431) and the Δ*yciB* strain (KR1432) did not confer abnormal cell shapes, but most of cells were significantly elongated, which was expected from the observation of the cell carrying yciB on the plasmid (Section 3.1.2).

Next, I investigated the cell morphology of *ΔrodZ* mutant cells expressing YciB from pUT18-*yciBFL* and other truncated versions of *yciB* (Figure 21). The elongated cells with the tapered end were observed with the overexpression of YciBFL. Similar cell shape was

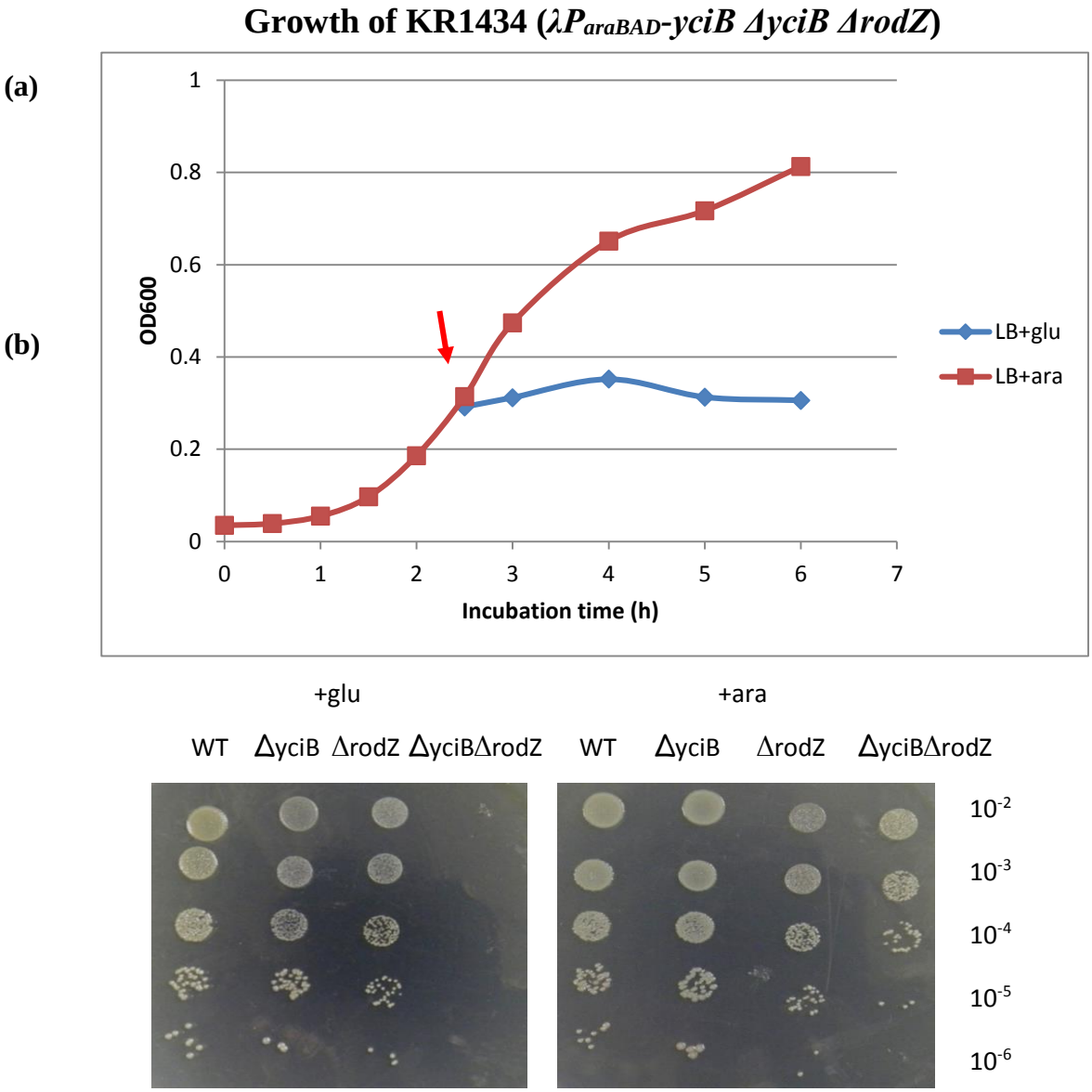

Figure 18: Growth of Δ*rodZ*Δ*yciB* mutant carrying an inducible yciB gene.

(a) KR1434 (*λP*$_{araBAD}$-*yciB ΔyciB ΔrodZ*) were cultured at 37 ºC in LB medium. At indicated time (arrow), the cultures were divided and 0.2 % L-arabinose or glucose were added. Aliquot of each culture were taken and OD600 were measured at indicated time.
(b) KR1431 (*λP*$_{araBAD}$-*yciB*), KR1432 (*λP*$_{araBAD}$-*yciB ΔyciB*), KR1433 (*λP*$_{araBAD}$-*yciB ΔrodZ*) and KR1434 (*λP*$_{araBAD}$-*yciB ΔyciB ΔrodZ*) were cultured at 37 ºC in LB medium until OD600 = ~ 0.5 and diluted in LB medium. Five micro litre of each diluent were spotted on LB agar plate.

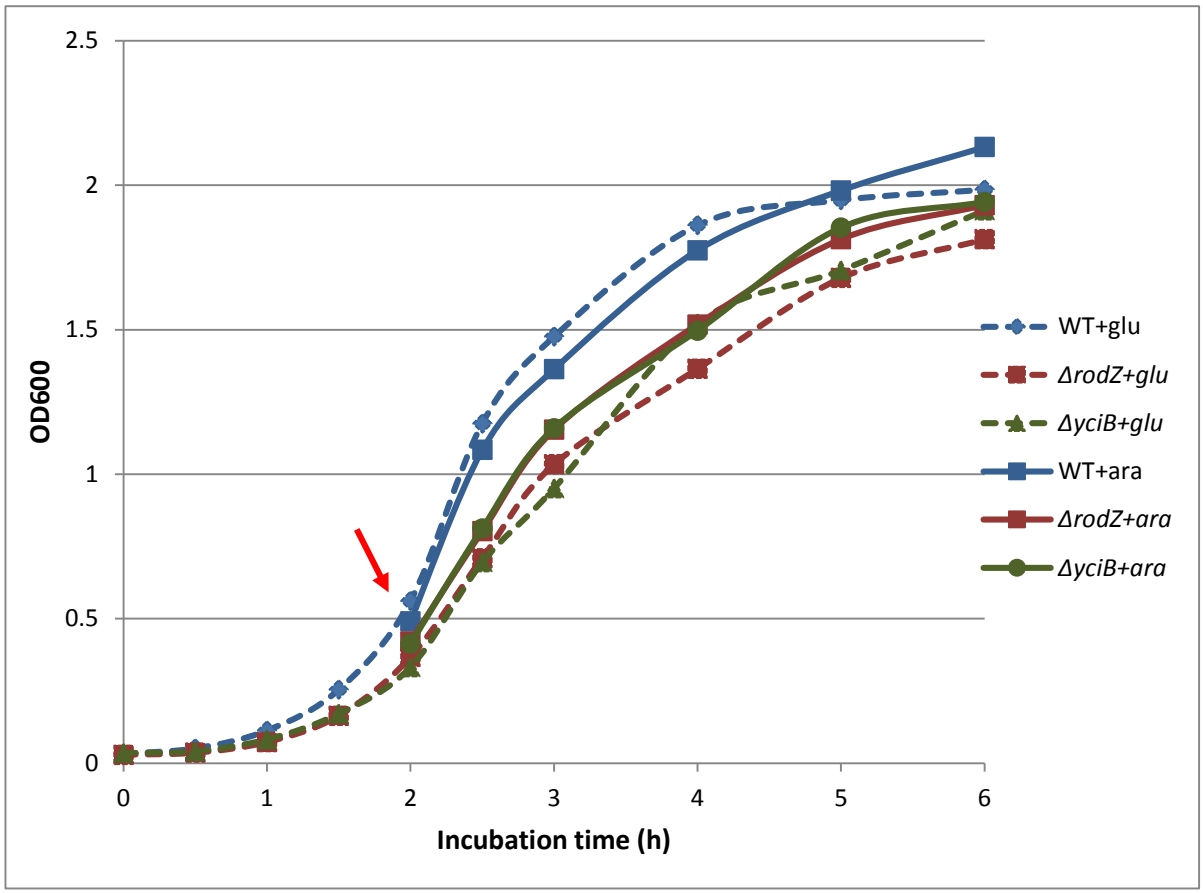

Figure 19: Growth of WT, Δ*rodZ* and Δ*yciB* mutants carrying an inducible yciB gene.

KR1431 (λP_{araBAD}-*yciB*), KR1432 (λP_{araBAD}-*yciB ΔyciB*) and KR1433 (λP_{araBAD}-*yciB ΔrodZ*) were grown at 37 ºC in LB medium. At indicated time (arrow), the cultures were divided and 0.2% L-arabinose or glucose were added. Aliquot of each culture were taken and OD600 were measured at indicated time. KR1431 (λP_{araBAD}-*yciB*): blue; KR1432 (λP_{araBAD}-*yciB ΔyciB*): green; KR1433 (λP_{araBAD}-*yciB ΔrodZ*): red. Solid (___) and dotted (----) lines indicate the culture with arabinose and glucose, respectively.

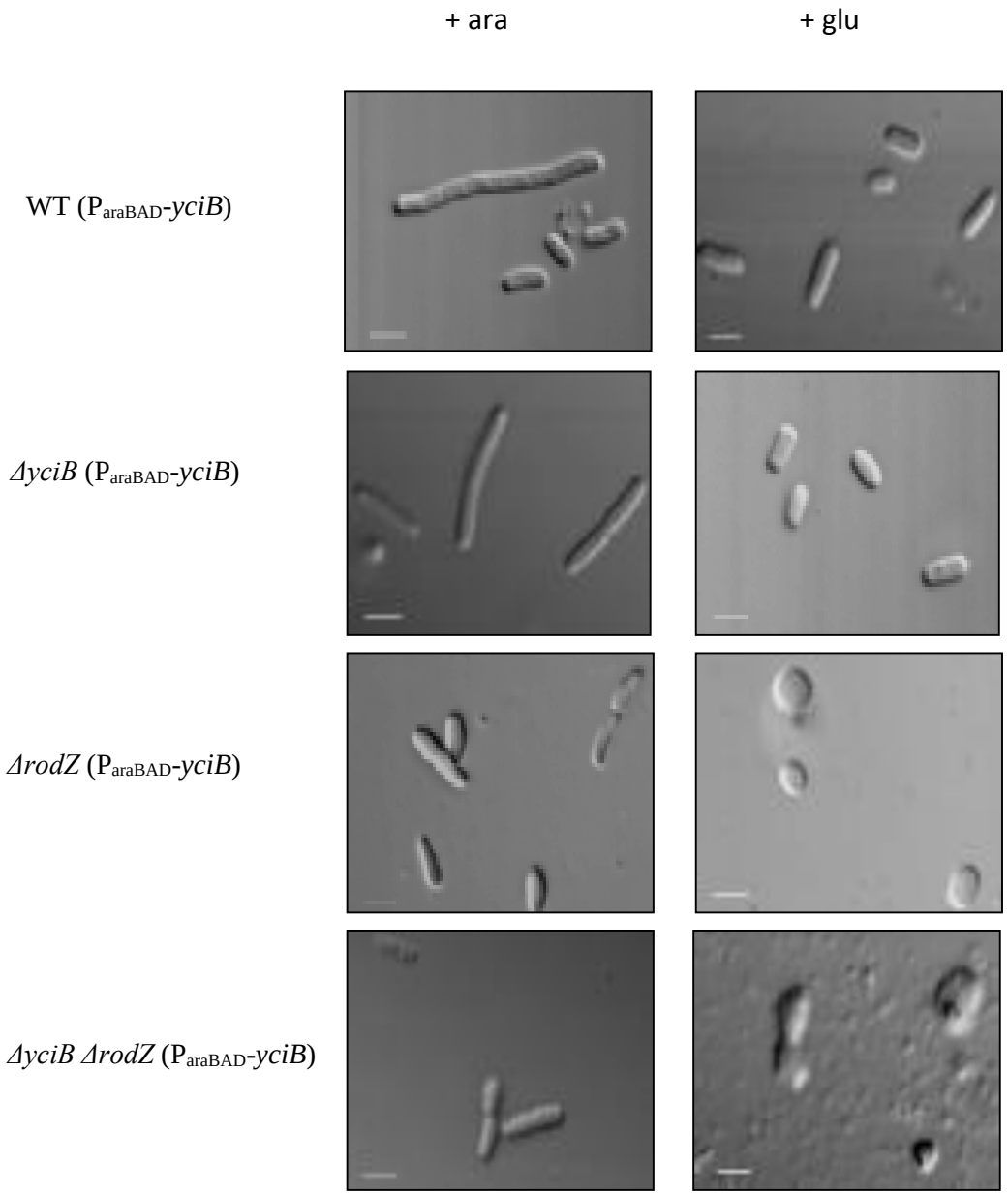

Figure 20: Cell morphology of WT, Δ*rodZ*, Δ*yciB* and Δ*rodZ*Δ*yciB* mutants carrying an inducible yciB gene.

Aliquots of the cell cultures in LB of KR1431 (*λP$_{araBAD}$-yciB*), KR1432 (*λP$_{araBAD}$-yciB ΔyciB*), KR1433 (*λP$_{araBAD}$-yciB ΔrodZ*) and KR1434 (*λP$_{araBAD}$-yciB ΔyciB ΔrodZ*) were taken after 1 hour induction or repression by 0.2% L-arabinose or glucose and fixed with 4% PFA. The samples were observed by microscope. Scale bar = 2 µm.

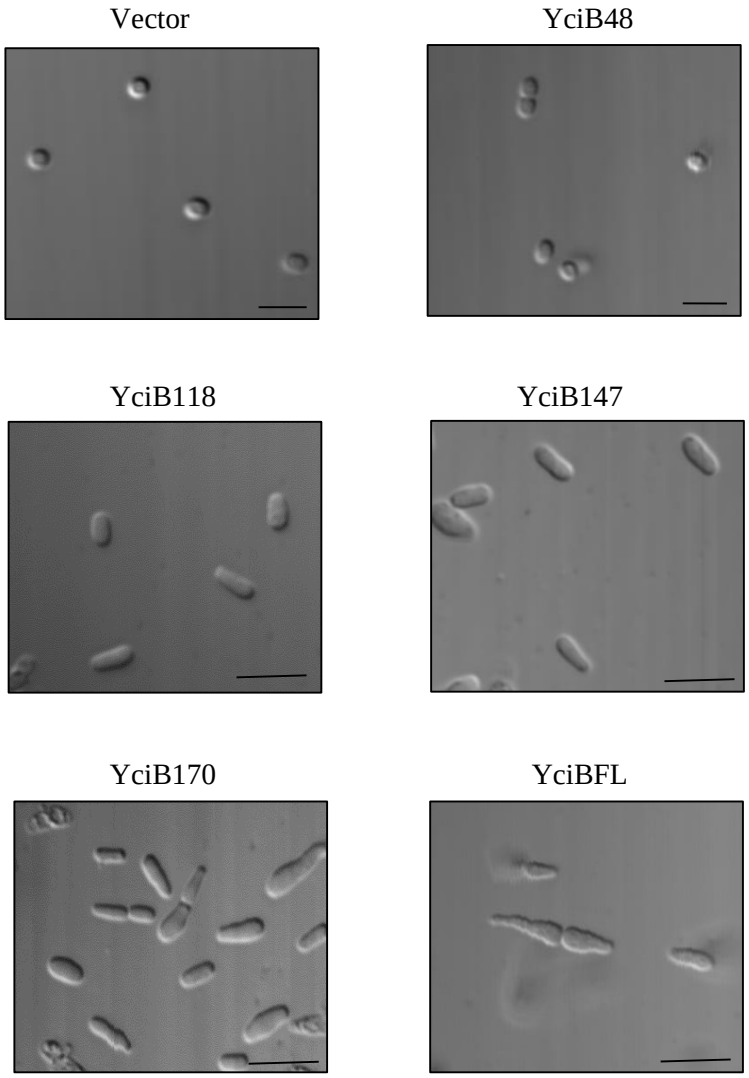

Figure 21: Suppression of the Δ*rodZ* mutant by overexpression of truncated versions of *yciB*.

Aliquots of the cell cultures in LB of KR1421 (*ΔrodZ*) carrying plasmid T18-*yciB* and its truncated variants were taken after 1 hour induction by 50 µM IPTG and fixed with 4% PFA. The samples were observed by microscope. Scale bar = 2 µm.

reported previously by Shiomi *et al*. (2013), in which the *ΔrodZ* cell harboured a *mreB* mutation. Meanwhile, YciB170 also suppressed the sphere shape of *ΔrodZ* mutant but the cells were shorter than by the full length of YciB. Moreover, overexpression of YciB147 and YciB118 suppressed the sphere shape of *ΔrodZ* mutant even lesser extent and YciB48 did not restore at all the sphere shape of *ΔrodZ* mutant.

3.3 Involvement YciB in cell division

Although YciB is not localized at the cell division site as most of proteins involved in cell division, BACTH analysis indicated that YciB also functionally interacts with some of division proteins. Recently, FtsZ, ZipA and some other proteins involved in cell division were shown to migrate through the cell and accumulate at the mid-cell when cell division starts (Vicente *et al*., 2006). Therefore, I examined the cellular localization of some of these division proteins.

3.3.1 YciB effects ZapA and ZipA localization at the septum site.

First, to investigate if YciB is involved in the localization of cell division proteins, I observed some cell division proteins fused with GFP in Δ*yciB* mutant and wild type cells using Olympus Fluoview FV1000-D system. For this purpose, I first used ASKA (Kitagawa *et al*., 2005) clones carrying *zapA* and *zipA* genes The *E. coli* strains to be examined were grown in LB medium containing appropriate antibiotics and 0.5 mM IPTG. I also observed the localization of ZapA and ZipA under induction and repression of YciB by using KR1432 (λP_{ara}-*yciB ΔyciB*) strain that expressing Zap-GFP or ZipA-GFP. The 0.2% arabinose or 0.2% glucose was added into the culture when the cell density reached at about ~0.2 of OD_{600}. The samples were collected after 1 hour induction or repression. Cells were fixed and treated as described in Materials and Methods.

The absence of YciB did not affect the localization of FtsZ and FtsA. On the contrary, ZapA protein was mostly localized at the cell pole instead of the division site in the absence of YciB. The cell pole localization of ZapA-GFP was also observed upon depletion of YciB in KR1432 (λP_{ara}-*yciB ΔyciB*) strain by adding glucose. While in the presence of arabinose, *yciB* was induced and ZapA-GFP was localized at the division sites of filamentous cells, which was caused by overproduction of ZapA (Figure 22). Here, I should note that the filamentation of the cell due to the overproduction of ZapA was not observed, which further indicates the role

of YciB in cell elongation described above. These findings indicated that YciB effects the localization of ZapA.

Next I examined the localization of ZipA-GFP in the *ΔyciB* mutant. As in the case of ZipA protein, in the absence of YciB, ZipA-GFP was not localized at the mid-cell but several foci of ZipA-GFP were observed along the shorter cell. This observation was consistent with strains that express ZipA-GFP from the chromosome integrated gene (Figure 23 and 24). The localization of ZipA-GFP and filamentation of the cell by overproduction of ZipA was also complemented by the induction of *yciB* gene. This study revealed that YciB is important for the septum site localization of ZipA, an essential divisome protein, although *yciB* gene is not essential in *E. coli*.

Finally, to avoid the possible effect of overproduction on the protein localization, I also used chromosome integrated strain for *zipA*, *ftsA* and *ftsZ* (Hale *et al*., 1997; Hale et la., 1999) and a minimal amount of IPTG to induce the corresponding fusion proteins. Again, ZipA-GFP expressed in a *ΔyciB* mutant was not localized at division site as in the wild type (Figure 24). As described above, the cell length of *ΔyciB* mutant is shorter than wild type indicating a defective synthesis of cell envelope. This might have caused a detection of ZipA very close to each other due to the short distance between the replicated nucleoids, in spite of its localization at the division site. Therefore, to examine this possibility, cells expressing ZipA-GFP was stained by DAPI and the location of ZipA relative to the chromosome was determined. In wild type cells almost all ZipA-GFP was observed only at the mid-cell and not overlapped with DAPI stained chromosomes. On the other hand, *ΔyciB* mutant cells showed ZipA-GFP not only between the nucleoids but also at the site of DAPI stained chromosomes. This clearly indicated that the localization or accumulation of ZipA to the cell division site was hindered in the *ΔyciB* mutant. We also examined the localization of FtsZ-GFP and FtsA-GFP produced in similar strains (DR120 (λP_{lac}*::gfpmut2-t-ftsA*) and CH75 (*λ*P_{lac}*::gfpmut2-t-ftsZ*)). The mid-cell localization of these proteins was not altered in *ΔyciB* mutant indicating that the absence of YciB does not hinder the Z-ring formation.

3.3.2 Regions of YciB required for the septum site localization of ZipA

Next, I investigated the complementation of truncated YciB in the ZipA localization at the septum site. I transformed the pKNT25-*yciBFL* and other truncated YciB variants into KR1412 (*ΔyciB::kan*^{s}) that containing pCA24N-*zipA*. For the ZipA localizaton, YciB seems

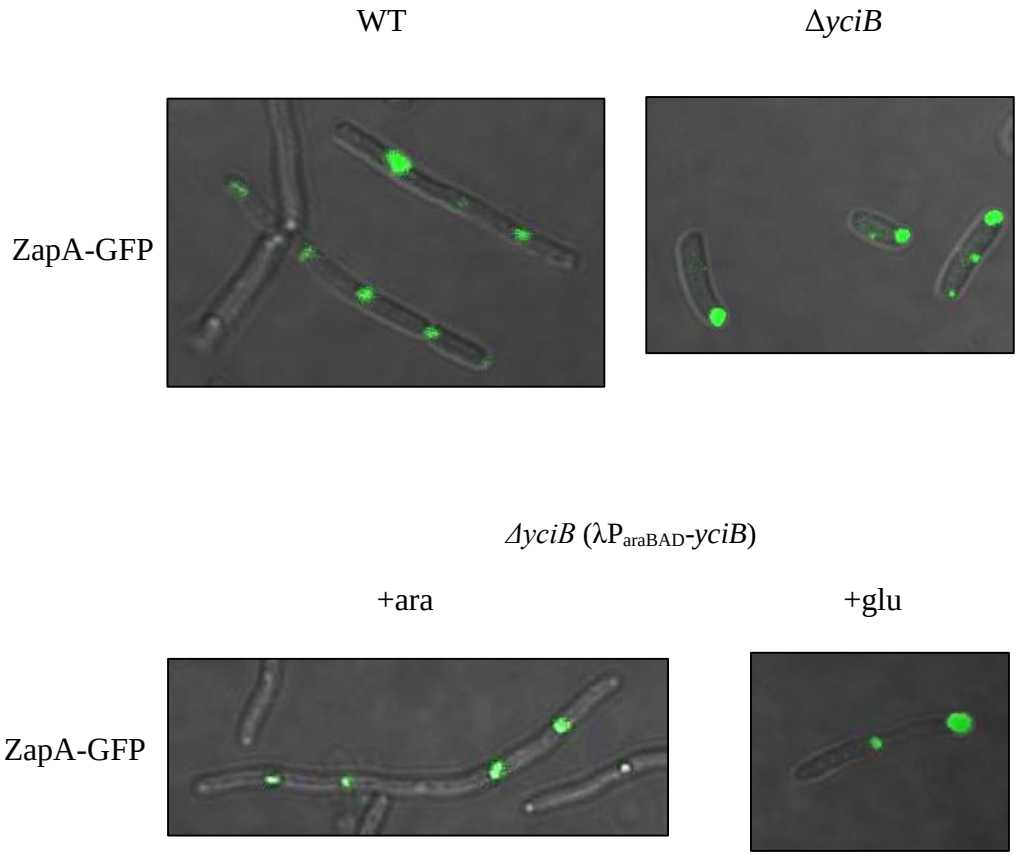

Figure 22: Localization of Zap-GFP in WT, Δ*yciB* mutant and *ΔyciB* (λP$_{araBAD}$-*yciB*).

Cells expressing ZapA-GFP from pCA24N were cultured in LB medium containing chloroamphenicol at 37 ^{o}C and induced with 0.5 mM IPTG. For *ΔyciB* (P$_{araBAD}$-*yciB*) strain, the culture was added with 0.2% arabinose or 0.2 % glucose for induction or repression of *yciB*. The samples were collected after 1 h induction or repression. The cells were fixed with 4 % PFA and observed by fluorescence microscope.

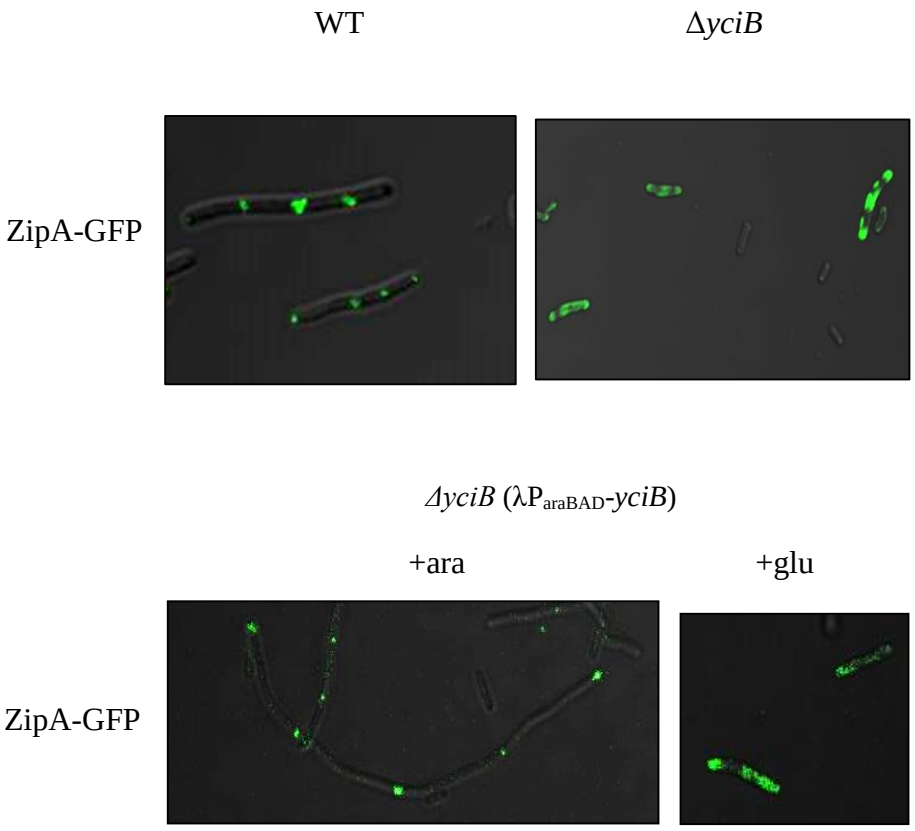

Figure 23: Localization of ZipA- GFP in WT, Δ*yciB* mutant and *ΔyciB* (λP$_{araBAD}$-*yciB*).

Cells expressing ZipA-GFP from pCA24N were cultured in LB medium containing chloroamphenicol at 37 ^{o}C and induced with 0.5 mM IPTG. For *ΔyciB* (P$_{araBAD}$-*yciB*) strain, the culture was added with 0.2% arabinose or 0.2 % glucose for induction or repression of *yciB*. The samples were collected after 1 h induction or repression. The cells were fixed with 4 % PFA and observed by fluorescence microscope.

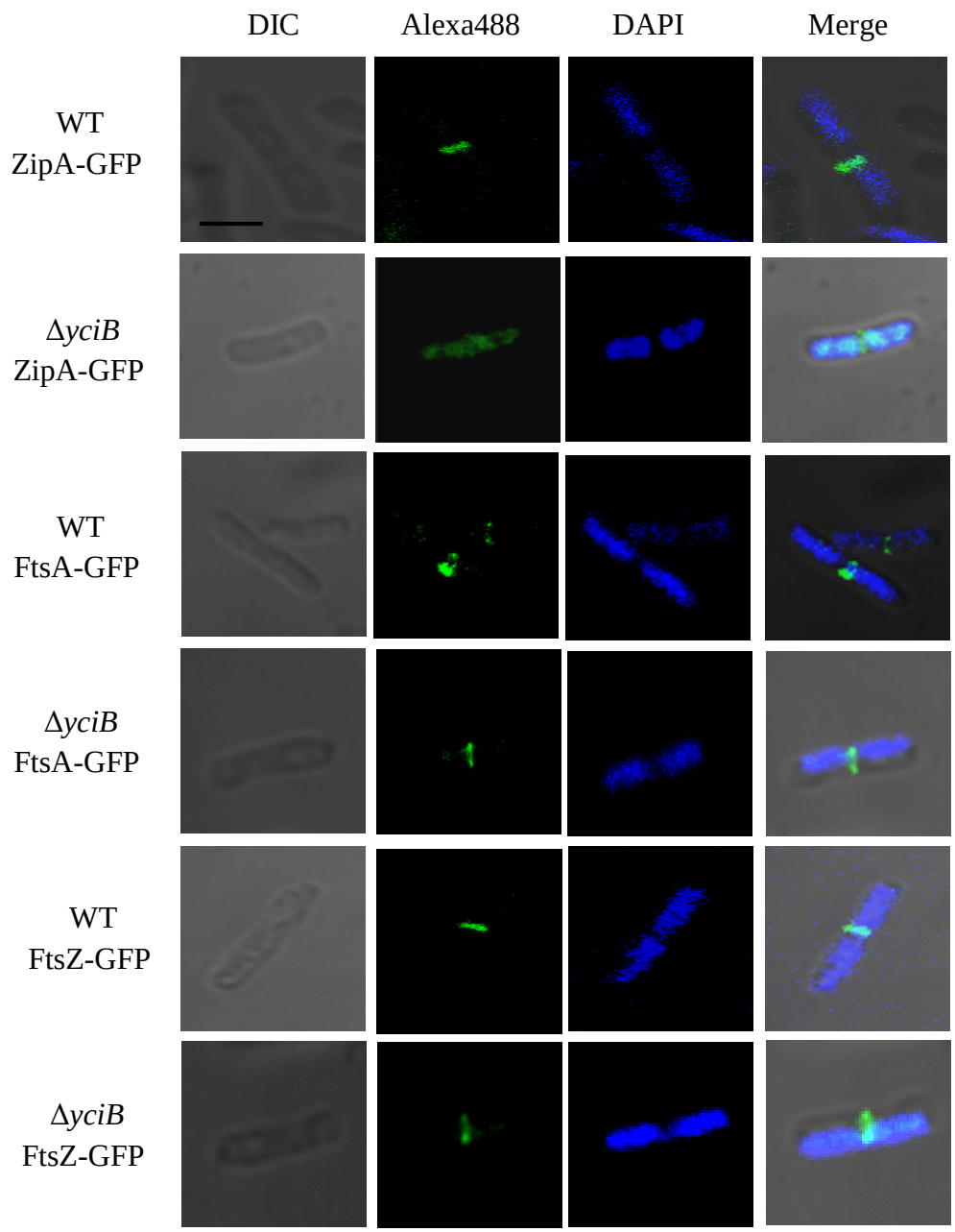

Figure 24: Localization of ZipA-GFP, FtsA-GFP and Fts-GFP in WT and Δ*yciB* mutant.

Cell expressing ZipA-GFP, FtsA-GFP and FtsZ-GFP from CH50 (λ P_{lac}*::zipA-gfpS65T*), DR120 (λP_{lac}*::gfpmut2-t-ftsA*) and CH75 (*λ*P_{lac}*::gfpmut2-t-ftsZ*), respectively, were cultured in LB medium containing ampicilin at 30 ^{o}C. The strain CH50 and DR120 were induced with 25 µM IPTG and CH75 was induced with 50 µM IPTG. Cell were fixed with 4% PFA, immunofluorescence stained using with anti-GFP and anti-rabbit conjugated with Alexa488. Cells were also DAPI stained using ProLong Diamond Antifade Mountant with DAPI and observed by fluorescence microscope. Scale bar = 2 µm.

not to require the C-terminal 9 amino acid residues and the last transmembrane domain since YciB170 and 147 could complement the loss of YciB. The cell length of these strains were much longer than the strains producing YciB118 and YciB48. The strains producing YciB118 partially complement the mislocalization of ZipA localization, but YciB48 did not complement at all (Figure 25).

3.3.4 YciB interacted with ZipA *in vitro*

Because YciB was shown to be important for ZipA and ZapA protein localization as well as in the support of *ΔrodZ* mutant, I finally examined the interaction between YciB and ZipA *in vitro*. S-His_6-tagged YciBFL, YciB117, YciB147, YciB118, YciB48 and MalG were expressed from plasmid pBADs. MalG was used as negative control since MalG did not interact with ZipA by BACTH analysis and its function is not related to cell elongation and cell division. The protein lysates were prepared using BugBuster-protein extraction reagent (Novagen) and purified by COSMOGEL His Accept (Nacalai). The purified proteins were mixed with T18-ZipA and applied on the column of Cosmogel His Accept. Eluents and flow-through of the samples were analysed on a 12.5% SDS-PAGE gel followed by Western Blotting analysis using HRP-conjugated S-protein and anti-CyaA (T18) antibody as probes to detect YciB (MalG) and ZipA, respectively. Chemiluminescent signal in protein bands was detected and quantified using a Fujifilm LAS1000 imaging system.

The results obtained clearly showed that YciB binds ZipA because most of T18-ZipA was detected in the eluent together with YciB but not in the flow-through fraction (Figure 26), which strongly indicates the participation of YciB in the cell division process. YciB170 and YciB148 also bound ZipA, while YciB118 and YciB48 did not.

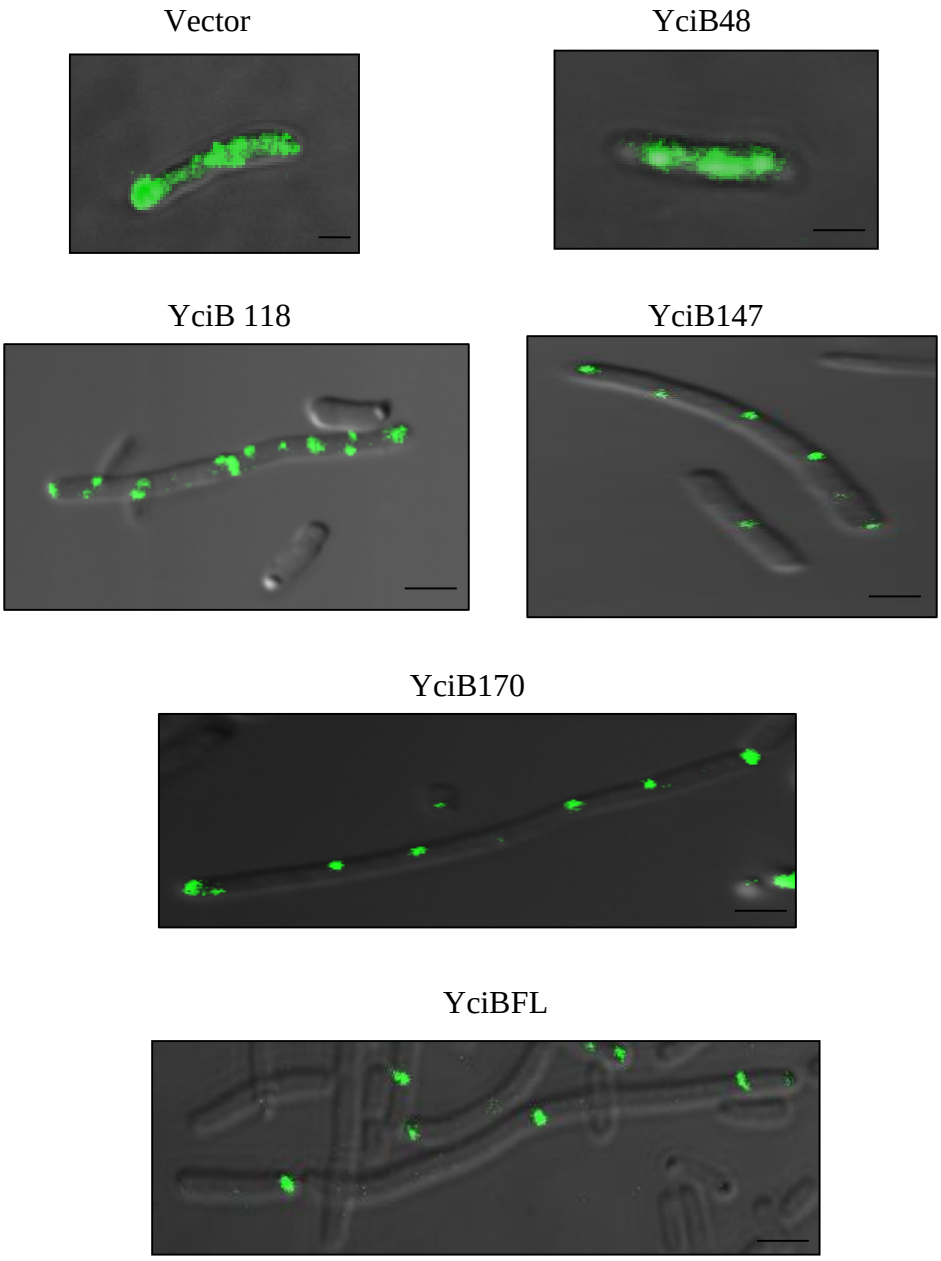

Figure 25: Complementation by truncated YciB variants of ZipA localization at the septum site.

Cells expressing ZipA-GFP from pCA24N in KR1412 (Δ*yciB::Kan*^{S} ^{c}) and carrying pKnT25-*yciBFL* or its truncated variants were cultured in LB medium containing kanamycin at 37 ºC and induced with 0.5 mM IPTG. Cells were fixed with 4% PFA and observed by fluorescence microscope. Scale bar = 2 µm.

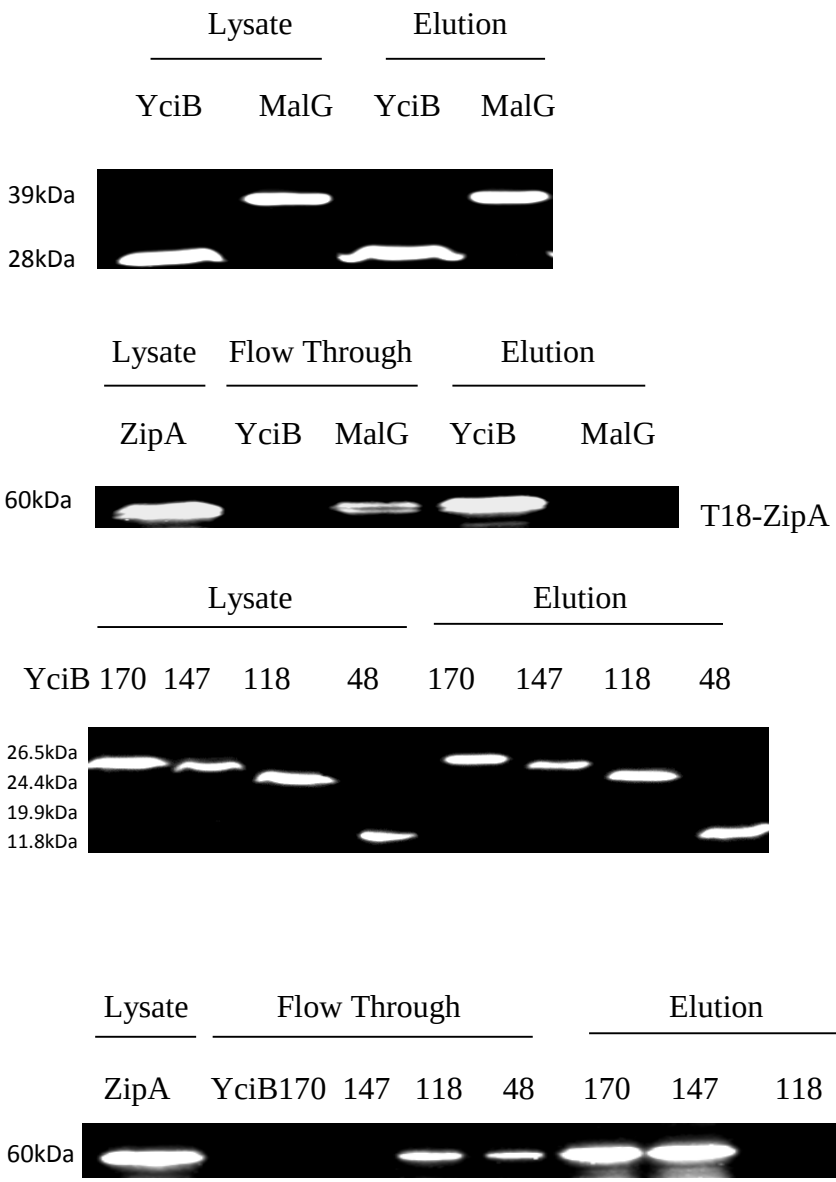

Figure 26: In vitro interaction between pBADs-YciBFL and its truncated variants and T18-ZipA.

Cell expressing the indicated proteins were cultured in LB medium containing ampicilin at 37 ^{o}C and induced with 0.2% arabinose or 0.5 mM IPTG. Proteins were extracted, purified and mixed for 30 min at RT. The interacted proteins were trapped with COSMOGEL His Accept and separated on SDS-PAGE. The protein were transferred to PVDF membrane and probed with S-protein or anti-CyaA (T18) antibody. The chemiluminescent signals were detected by LAS1000 imaging system.

4. DISCUSSION

4.1 Characterization of YciB

The gene *yciB* in *E. coli* has not been well investigated and its function remained unknown. It was reported that Δ*yciB* mutation was responsible to the reduced biofilm formation (Niba *et al.*, 2007) and more recently, that the Δ*yciB* mutant was sensitive to bicyclomycin, an inhibitor of transcription termination factor rho (Tran *et al.*, 2011). However, the *ispA*, a homologue of *yciB* in *Shigella flexneri*, was reported to play a role in cell division and intracellular spreading (Mac Siomoin *et al.*, 1996). Therefore, I aimed to reveal the cellular function of *yciB* and my study was focused on its involvement in the cell elongation and cell division processes.

In *E. coli*, Δ*yciB* mutation reduced the growth rate, although *yciB* is not essential for the cell growth. I have also analyzed various phenotypes of the Δ*yciB* mutant and found that the cell length of Δ*yciB* mutant was shorter than the WT and its cell wall strength was weaker, which indicated the involvement of YciB in cell elongation and probably defective in membrane integrity. On the other hand, an excess of YciB tended to elongate the cell and the overexpression of *yciB* was harmful to the cell, leading to the cell death in the end. The latter phenotype was severer in Δ*yciB* mutant; most of the cells appeared with empty regions at the pole and the division site of the cell. This observation seemed to indicate that the cell death upon overexpression of *yciB* was caused by the leakage of the newly made cell wall at the cell division site and that YciB has a role in proper peptidoglycan synthesis at the cell division site. In addition, some cells overproducing YciB also showed abnormality in chromosome segregation, which seemed to indicate that YciB might be involved in chromosome segregation. The mislocalization of ZipA (Section 3.3.1) in the absence of YciB might support this idea, since ZipA is required to recruit FtsK, a cell division protein important for the chromosome segregation (Hale and de Boer, 2002), to the septum site.

Next, I investigated the protein-protein interaction between YciB and cell elongation and cell division proteins using BACTH system. YciB was found to interact with many proteins in the elongasome (elongation complex) such as MurG, RodA and RodZ, and also with various cell division proteins like FtsB, FtsQ, ZapA and ZipA. These results further indicated that YciB is also involved in cell division, probably has a role in the synthesis of peptidoglycan at the division site, which corresponds well with the report on its homologue in *Shigella flexneri*, *ispA*, that the mutant of *ispA* was defective in cell division leading to the formation of long

filamentous shape lacking septa (Mac Siomon *et al.,* 1996). However, YciB interacted with many proteins involved in cell elongation. This might indicate that YciB associates with the elongasome as well as divisome.

4.2 Role of YciB in cell elongation and division

The sensitivity of Δ*yciB* mutant to A22 may present an evidence for the requirement of YciB in cell elongation. In *E. coli,* A22 disturbed subcellular localization of MreB and caused a rod-to-sphere shape conversion (Iwai *et al.*, 2002). The involvement of YciB in cell elongation was also indicated by previous result showing a genetic interaction between *yciB* and *rodZ* (Niba *et al.*, 2010). The *rodZ* gene is important to maintain the rod-type cell morphology and the Δ*rodZ* mutant shows a spherical cell shape. In this study, I showed that the depletion of YciB made the Δ*rodZ* mutant unable to grow and the cell was lysed in the end. These analyses has proved that Δ*yciB*Δ*rodZ* double mutant is synthetically lethal. There are several proteins required for the maintenance of rod shape in *E. coli* such as MreB, MreC, MreD, RodA and RodZ. All these proteins are essential except RodZ, which seems to indicate that RodZ has a partner that compensates the loss of RodZ to survive. The synthetic lethality of Δ*yciB*Δ*rodZ* double mutation suggests that YciB is such protein. I speculate that YciB provides cell a mean to elongate up to the critical length before the cell division occurs and PIPS (PBP3-independent peptidoglycan synthesis) could be the mechanism to support the viability of ΔrodZ mutant. The PIPS performs the lateral synthesis of peptidoglycan at the mid-cell prior to cell division. If the depletion of YciB renders the cell defective or inefficient in PIPS, then the Δ*rodZ*Δ*yciB* mutant would become unable to increase the cell wall and hence to support the cell growth, because RodZ is required in the cell elongation process by the lateral peptidoglycan synthesis with PBP2. Previously, it was reported that the viability of *mre*$^{-}$ cells was recovered by overexpression of FtsZ, which allows mutants to grow and divide as sphere cells (Bendezu and de Boer., 2008), and that *ftsZ* and *zipA* are also involved in PIPS (Varma *et al.*, 2007). Considering these reports, I suspected that YciB might contribute to PIPS and in this respect YciB is involved both in cell elongation especially in peptidoglycan synthesis. Furthermore, the shorter cell length of Δ*yciB* mutant and the YciB localization which is throughout the membrane would support this hypothesis.

I also investigated the localization in Δ*yciB* mutant of some proteins involved in cell division by fluorescence microscopy, and found that the mid-cell localization of ZipA and

ZapA proteins was disturbed in Δ*yciB* mutant. These proteins bind FtsZ and stabilize the FtsZ-ring. Polar localization of ZapA might be caused by the delay of peptidoglycan synthesis in the absence of YciB. Normally, when rod-shaped bacteria divide, each daughter cell invariably inherits an 'old' pole from its mother and a 'new' pole freshly formed at the site of division. Therefore, a cell division protein that is stably bound to the septum ring before the cytokinesis could result in localizing at a new pole after cell separation (Figure 27) (Laloux and Jacobs-Wagner, 2014). ZapA might be retained longer at the "new" pole before the next cell cycle initiates because of the slow growth of Δ*yciB* mutant. Alternatively, the excess ZapA that has not properly been recruited at the septum site has increased in the mutant and such overproduced ZapA tends to be localized at the pole. Polar localization of overproduced proteins was also observed in case of other proteins.

I also found that ZipA-GFP was not focused at the septum site but observed at various parts in the Δ*yciB* mutant. Furthermore, the wild type cell overproducing ZipA, KR0401/pCA24N-*zipA*, is defective in cell division and formed filamentous cells as previously reported (Hale and de Boer, 1997), while the Δ*yciB* mutant carrying pCA24N-*zipA* appeared much shorter in length. This observation indicated that the shorter filament of Δ*yciB* mutant with overexpressing ZipA might be due to the inhibition/reduction of lateral PG synthesis near the midcell due to the mislocalization of ZipA. ZipA is required in the elongation of cell envelope near the cell division site (PIPS). On the other hand, the FtsZ localization was not affected in the absence of YciB. Microscopic analysis of FtsA-GFP also showed the mid-cell localization of this protein, indicating that FtsA properly functions by interacting with FtsZ in Δ*yciB* mutant. Possible reason for the mid-cell localization of FtsZ in Δ*yciB* mutant could be the functional redundancy between ZipA and FtsA as well as between ZapA and ZapB. These proteins work at the septum site and stabilize the assembled Z-ring (Pichoff and Lutkenhaus, 2002; Mohammadi *et al.*, 2009).

My study also showed that YciB directly binds to ZipA that possesses only a short periplasmic peptide (6 a.a) at the N terminus. Therefore, YciB might be a molecule connecting ZipA and the periplasmic peptidoglycan synthesis machinery. This observation also supports the above hypothesis that YciB participates in PIPS, because ZipA is required for PIPS together with FtsZ (Potluri *et al.*, 2012).

For the ZipA localization and binding, YciB seems not to require the C-terminal 9 amino acid residues but this peptide conferred YciB a toxic effect upon overexpression. Further

deletion of the C-terminal region containing TM domains reduced or eliminated the activity of YciB in the mid-cell localization of ZipA and the elongation of spherical cell of the Δ*rodZ* mutant. The mechanisms in which YciB assists ZipA to localize at the septum site in the cell division process as well as the relation with the molecular structure of YciB remain to be elucidated. In this study, however, I could find that YciB interacts with RodZ and ZipA, as well as with various cell elongation and division proteins by BACTH system, which might suggest that YciB plays some roles in transition from the cell elongation to cell division (Figure 28).

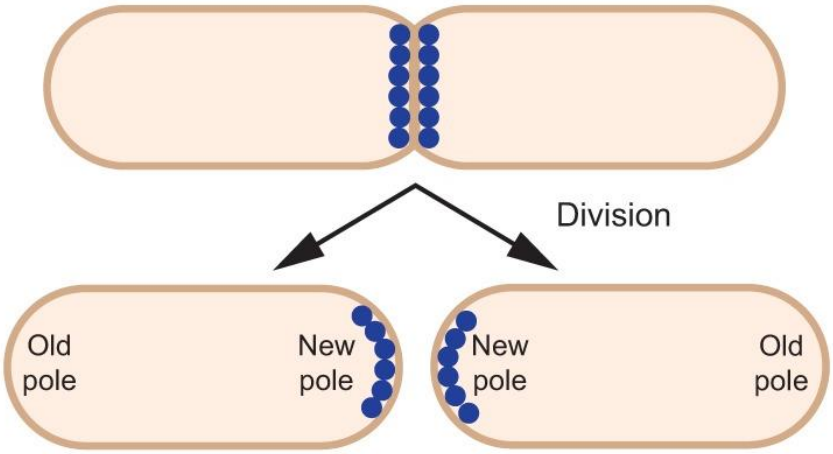

Figure 27: Localization of polar proteins resulting from cell division.

Proteins stably localized at the midcell before cell division remain associated with the newly formed cell poles in the progeny (Laloux and Jacobs-Wagner, 2014)

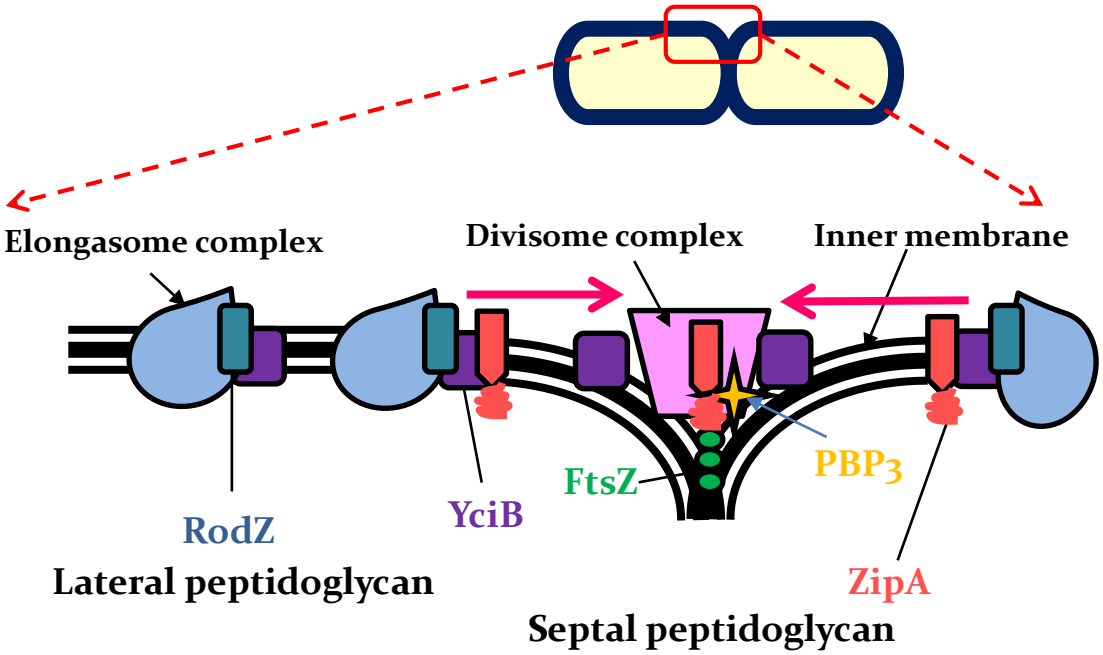

Figure 28: Model illustrating the interaction of YciB with cell elongation and division proteins.

YciB interacts with elongasome complex including RodZ in order to promote lateral peptidoglycan synthesis. At the same time, YciB binds to ZipA and assists its movement to the division site, which will lead to the septal peptidoglycan synthesis together with divisome complex.

4.3 Mechanisms of suppressing the sphere phenotype of the *ΔrodZ* mutant by *yciB* overexpression

As described in previous reports, Δ*rodZ* mutants exhibited sphere shape instead of the rod-type cell indicating its role in lateral peptidoglycan synthesis. Shiomi *et al.* (2009) reported that the Δ*rodZ* sphere cell still retains a defined single cell polarity and elongates laterally, but probably with a shortened central cylinder of the normal rod cell. It was found that an overproduction of ZipA in the Δ*rodZ* cell by a promoter mutation suppresses the spherical cell morphology and authors reasoned that the mutation delays the completion of septation and provides the cell an extra time to elongate laterally (Shiomi and Niki, 2013). This study showed that the overexpression of YciB also suppressed the Δ*rodZ* sphere shape and forms an irregular rod–type cell. Excess YciB itself tended to increase the cell length suggesting that the elongated cells have extra lateral peptidoglycan. The observation of DAPI-stained cells showed that the longer cell does not contain extra copies of the chromosome compared to WT. This observation was different from filamentous cells elongated by overexpression of ZipA or some other cell division proteins, where the cell elongation was caused by inhibition of cell division and one filamentous cell contains more than 4 replicated chromosomes (Hale and de Boer, 1997). Therefore, I guess that extra synthesis of peptidoglycan at the division site by overexpression of YciB elongated the Δ*rodZ* sphere cell. However, these cells lack the general synthesis of lateral peptidoglycan in the absence of RodZ and result in the abnormal rod-type or tapered cell shape. Similar phenotype was reported by Shiomi *et al.* (2013) for *mreB* suppressor mutants of *ΔrodZ*. These observations seem to indicate that proteins in elongation complex as well as in divisome need to coordinate to maintain the rod-type morphology and YciB plays an important role in cell morphology, although the gene *yciB* is not essential in *E. coli*.

4.4 Well-regulated expression of YciB is important for the normal cell growth

In *E. coli*, *yciB* gene is located between *yciA* and *yciC* and this genetic context is conserved in most of gammaproteobacteria and some species in alpha- and beta- proteobacteria but no apparent homologue of *yciB* exists in Gram-positive bacteria. The gene *yciB* and *yciC* seem to be transcribed at a very low level, while *yciA* is expressed at a higher level from a separate promoter (Li, 2011). This low level expression of *yciB* and *yciC* probably indicates that a tight regulation is working on them to avoid overexpression. The correct level of expression seems to be very important for YciB to function properly and not to impose any

harm on the cell. Many incidents encountered during the course of this study suggested this strict regulation in expression of the gene. In the BACTH analysis, pUT18-*yciBFL* was expressed at a lower level than C-terminally truncated YciB versions, probably to keep the cell alive. It was also shown that YciB expressed from the multi-copy plasmid pBADs cannot complement the sensitivity of *Δ*yciB mutant to A22, but the chromosome-integrated *yciB* could suppress the sensitivity to a certain extent. Previously, Hale *et al.* (2000) reported the failure of wild-type ZipA expressed from a plasmid in complementing the *ts* mutation of *zipA*. These results indicate that the well-coordinated expression of genes involved in cell elongation and division is important for the cell cycles to proceed smoothly.

4.5 Perspective and future works

Cell elongation and division are fundamental processes of living organisms and many essential and accessory genes are involved. However, the mechanisms and precise function of the genes remain unclear. This study revealed that YciB participates both in cell elongation and cell division, but unlike conventional Fts proteins it is not localized at the division site. In order to clarify the function of YciB, it will be necessary further to investigate the interaction with genes that are involved in these cellular processes but different from *fts* genes, such as those in Min system and genes encoding outer membrane proteins. Protein-protein interactions indicated by TH analysis should be confirmed by *in vitro* experiments. Also more biochemical work is necessary to clarify the role of YciB in peptidoglycan synthesis.

Although *E. coli* has widely been studied from various aspects over the years, there are still many genes that are not functionally classified. Adding to characterized cell elongation and cell division genes, still many unidentified genes are probably participating in these fundamental cellular processes. Recently, YmgF and Blr, products of uncharacterized genes, were reported to interact with the divisome (Karimova *et al.*, 2009; 2012). While, two DedA family proteins were reported to participate in export of the periplasmic amidases AmiA and AmiC that are required for normal cell division and envelope integrity (Sikdar *et al.*, 2013). We also found that *yhcB* encoding an inner membrane protein functionally interacts with *rodZ* (Li *et al.*, 2012). In order to elucidate the mechanisms of cell elongation and division processes, further characterization of these genes would be necessary.

5. REFERENCES

Addinall SG, Lutkenhaus J. 1996. FtsZ ring formation in Fts mutants. J. Bacteriol. **178(13):**3877-3884.

Baba T, Ara T, Hasegawa M, Takai Y, Okumura Y, Baba M, Datsenko KA, Tomita M, Wanner BL, Mori H. 2006. Construction of *Escherichia coli* K-12 in-frame, single-gene knockout mutants: the Keio collection. Mol. Syst. Biol. **2:**2006.0008.

Bendezu FO, de Boer PAJ. 2008. Conditional lethality, division defects, membrane involution and endocytosis in *mre* and *mrd* shape mutant shape mutants of *Escherichia coli*. J. Bacteriol. **190(5):**1792-1811.

Bendezu FO, Hale CA, Bernhardt TG, de Boer PA. 2009. RodZ (YfgA) is required for proper assembly of the MreB actin cytoskeleton and cell shape in *E. coli*. EMBO J. **28(3):**193-204.

Blattner, FR, Plunkett G, Bloch CA, Perna NT, Burland V, Riley M, Collado-Vides J, Glasner JD, Rode CK, Mayhew GF, Gregor J, Davis NW, Kirkpatrick HA, Goeden MA, Rose DJ, Mau B, Shao Y. 1997. The complete genome sequence of *Escherichia coli* K-12. Science. **277(5331):**1453-62.

Boyd D, Weiss DS, Chen JC, Beckwith J. 2000. Towards single-copy gene expression systems making gene cloning physiologically relevant: lambda InCh, a simple *Escherichia coli* plasmid-chromosome shuttle system. J. Bacteriol. **182:**842–847.

Cabeen MT, and Jacobs-Wagner C. 2005. Bacterial cell shape. Nat. Rev. Microbiol. **3:**601-610.

Chen JC, Weiss DS, Ghigo JM, Beckwith J. 1999. Septal localization of FtsQ, an essential division protein in *Escherichia coli*. J. Bacteriol. **181(2):**521-530.

Cronan JE. 2006. A family of arabinose-inducible *Escherichia coli* expression vectors having pBR322 copy control. Plasmid. **55(2):**152-157.

Datsenko KA, Wanner BL. 2000. One-step inactivation of chromosomal genes in *Escherichia coli* K-12 using PCR products. Proc. Natl. Acad. Sci. U. S. A. **97:**6640–6645.

de Boer PAJ, Crossley RE, Hand AR, Rothfield LI. 1991. The MinD protein is a membrane ATPase required for the correct placement of the *Escherichia coli* division site. EMBO J. **10(13):**4371-80.

Durand-Heredia JM, de Carlo S, Lesser CF, Janakiraman A. 2011. Identification and characterization of ZapC, a stabilizer of the FtsZ ring in *Escherichia coli*. J. Bacteriol. **193(6):**1405-1413.

Edwards DH, Errington J. 1997. The Bacillus subtilis DivIVA protein targets to the division septum and controls the site specificity of cell division. Mol. Microb. **24(5):**905-915.

Egan AJF, Vollmer W. 2013. The physiology of bacterial cell division. Ann. N. Y. Acad.Sci. **1277:**8–28.

Fields S, Song O. 1989. A novel genetic system to detect protein-protein interactions. Nature**. 340(6230):**245–246.

Gan X, Kitakawa M, Yoshino K, Oshiro N, Yonezawa K, Isono K. 2002. Tag-mediated isolation of yeast mitochondrial ribosome and mass spectrometric identification of its new component. Eur. J. Biochem. **269(21):**5203-5214.

Geissler B, Elraheb D, Margolin W. 2003. A gain-of-function mutation in *ftsA* bypasses the requirement for the essential cell division gene *zipA* in *Escherichia coli*. Proc. Natl. Acad. Sci. USA. **100(7):**4197-4202.

Hale CA, de Boer PAJ. 1997. Direct binding of FtsZ to ZipA, an essential component of the septal ring structure that mediates cell division in *E. coli*. Cell. **88:**175–185.

Hale CA, de Boer PAJ. 1999. Recruitment of ZipA to the septal ring of *Escherichia coli* is dependent on FtsZ and independent of FtsA. J. Bacteriol. **181:**167-176.

Hale CA, de Boer PAJ. 2002. ZipA is required for recruitment of FtsK , FtsQ , FtsL , and FtsN to the septal ring in *Escherichia coli*. J. Bacteriol. **184:**2552–2556.

Hale CA, Rhee AC, de Boer PAJ. 2000. ZipA-induced bundling of FtsZ polymers mediated by an interaction between C-terminal domains. J. Bacteriol. **182:**5153–5166.

Hale CA, Shiomi D, Liu B, Bernhardt TG, Margolin W, Niki N, de Boer PAJ. 2011. Identification of *Escherichia coli* ZapC (YcbW) as a component of the division apparatus that binds and bundles FtsZ polymers. J. Bacteriol. **193:**1393-1404.

Hill NS, Buske PJ, Shi Y, Levin PA. 2013. A moonlighting enzyme links *Escherichia coli* cell size with central metabolism. PLOS Gen. **9(7):**e1003663.

Hochuli E, Bannwarth W, Döbeli H, Gentz R, Stüber D. 1988. Genetic Approach to Facilitate Purification of Recombinant Proteins with a Novel Metal Chelate Adsorbent. Biotech. **6 (11):**1321–1325.

Hsieh CW, Lin TY, Lai HM, Lin CC, Hsieh TS, Shih YL. 2010. Direct MinE-membrane interaction contributes to the proper localization of MinDE in *E. coli*. Mol. Microbiol. **75(2):**499-512.

Hu ZL, Lutkenhaus J. 1999. Topological regulation of cell division in *Escherichia coli* involves rapid pole-to-pole oscillation of the division inhibitor MinC under the control of MinD and MinE. Mol. Microbiol. **34:**82–90.

Huberts DHEW, van der Klei IJ. 2010. Moonlighting proteins: An intriguing mode of multitasking. BBA-Mol. Cell Res. **1803(4):**520-525.

Ishino Y, Shinagawa H, Makino K, Tsunasawa S, Sakiyama F, Nakata A. 1986. Nucleotide sequence of the lig gene and primary structure of DNA ligase of *Escherichia coli*. Mol.Gen.Genet. **204:**1-7.

Iwai N, Nagai K, Wachi M. 2002. Novel S-benzylisothiourea compound that induces spherical cells in *Escherichia coli* probably by acting on a rod-shape-determining protein(s) other than penicillin-binding protein 2. Biosci. Biotechnol. Biochem. **66:**2658-2662.

Jones LJ, Carballido-Lopez R, and Errington J. 2001. Control of cell shape in bacteria: helical, actin-like filaments in *Bacillus subtilis*. Cell. **10:**4913-922.

Karimova G, Davi M, Ladant D. 2012. The β-lactam resistance protein Blr, a small membrane polypeptide, is a component of the *Escherichia coli* cell division machinery. J. Bacteriol. **194:**5576–5588.

Karimova G, Pidoux J, Ullmann A, Ladant D. 1998. A bacterial two-hybrid system based on a reconstituted signal transduction pathway. Proc. Natl. Acad. Sci. U. S. A. **95:**5752–5756.

Karimova G, Robichon C, Ladant D. 2009. Characterization of YmgF, a 72-residue inner membrane protein that associates with the *Escherichia coli* cell division machinery. J. Bacteriol. **191:**333–346.

Karp PD, Keseler IM, Shearer A, Latendresse M, Krummenacker M, Paley SM, Paulsen I, Collado-Vides J, Gama-Castro S, Peralta-Gil M, Santos-Zavaleta A, Peñaloza-Spínola MI, Bonavides-Martinez C, Ingraham J. 2007. Multidimensional annotation of the *Escherichia coli* K-12 genome. Nucleic Acids Res. **35(22):**7577-90.

Kippert F. 1995. A rapid permeabilization procedure for accurate quantitative determination of beta-galactosidase activity in yeast cells. FEMS Microbiol. Lett. **128:**201-206.

Kitagawa M, Ara T, Arifuzzaman M, Ioka-Nakamichi T, Inamoto E, Toyonaga H, Mori H. 2005. Complete set of ORF clones of *Escherichia coli* ASKA library (a complete set of *E. coli* K-12 ORF archive): unique resources for biological research. DNA Res. **12:**291–299.

Kruse T, Bork-Jensen J, Gerdes K. 2005. The morphogenetic MreBCD proteins of *E. coli* form an essential membrane bound complex. Mol. Microbiol. **55:**78-89.

Laloux G, Jacobs-Wagner C. 2014. How do bacteria localize proteins to the call pole?. J Cell Sci. **0:**1-9.

Li G, Hamamoto K, Kitakawa M. 2012. Inner Membrane Protein YhcB Interacts with RodZ Involved in Cell Shape Maintenance in *Escherichia coli*. ISRN Molecular Biology 2012:doi:10.5402/2012/304021.

Li G. 2012. Ph.D thesis. Kobe University, Kobe, Japan.

Lowe J, van den EF, Amos LA. 2004. Molecules of the bacterial cytoskeleton. Annu. Rev. Biophys. Biomol. Struct. **33:**177-198.

Mac Síomóin RA, Nakata N, Murai T, Yoshikawa M, Tsuji H, Sasakawa C. 1996. Identification and characterization of *ispA*, a *Shigella flexneri* chromosomal gene essential for normal in vivo cell division and intercellular spreading. Mol. Microbiol. **19:**599–609.

Miller JH. 1972. Experiments in molecular genetics. Cold Spring Harbor Laboratory Press, Cold Spring Harbor N. Y.

Mohammadi T, Karczmarek M, Bouhss A, Mengin-Lecreulx D, den Blaauwen T. 2007. The essential peptidoglycan glycosyltransferase MurG forms a complex with proteins involved in lateral envelope growth as well as with proteins involved in cell division in *Escherichia coli*. Mol. Microbiol. **65:**1106–1121.

Mohammadi T, Ploeger GE, Verheul J, Comvalius AD, Martos A, Alfonso C, van Marle J, Rivas G, den Blaauwen T. 2009. The GTPase activity of *Escherichia coli* FtsZ determines the magnitude of the FtsZ polymer bundling by ZapA in vitro. Biochem. **48:** 11056–11066.

Moller-Jensen J, Lowe J. 2005. Increasing complexity of the bacterial cytoskeleton. Cell. Biol. **17(1):**75-81.

Nanninga N. 1991. Cell division and peptidoglycan assembly in *Escherichia coli*. Mol Microbiol. **5(4):**791-5.

Niba ET, Li G, Aoki K, Kitakawa M. 2010. Characterization of *rodZ* mutants: RodZ is not absolutely required for the cell shape and motility. FEMS Microbiol Lett. **309(1):**35-42.

Niba ETE, Naka Y, Nagase M, Mori H, Kitakawa M. 2007. A genome-wide approach to identify the genes involved in biofilm formation in *E. coli*. DNA Res. **14:**237–246.

Nijman MBS. 2011. Synthetic lethality: General principles, utility and detection using genetic screens in human cells. FEBS Lett. **585(1):**1-6.

Perna NT, Plunkett G, Burland V, Mau B, Glasner JD, Rose DJ, Mayhew GF, Evans PS, Gregor J, Kirkpatrick HA, Hackett J, Klink S, Boutin A, Shao Y, Miller L, Grotbeck EJ, Davis NW, Lim A, Dimalanta ET, Potamousis KD, Apodaca J, Anantharaman TS, Lin J, Yen G, Schwartz DC, Welch RA, Blattner FR. 2001. Genome sequence of enterohaemorrhagic *Escherichia coli* O157:H7. Nature. **409:**529-533.

Pichoff S, Lutkenhaus J. 2002. Unique and overlapping roles for ZipA and FtsA in septal ring assembly in *Escherichia coli. EMBO J.* ***21(4):****685-693.*

Potluri L-P, Kannan S, Young KD. 2012. ZipA is required for FtsZ-dependent preseptal peptidoglycan synthesis prior to invagination during cell division. J. Bacteriol. **194:**5334–5342.

Rueda S, Vicente M, Mingorance J. 2003. Concentration and assembly of the division ring proteins FtsZ, FtsA and ZipA during the *Escherichia coli* cell cycle. J. Bacteriol. **185:**3344–3351.

Shih YL, Le T, Rothfield L. 2003. Division site selection in *Escherichia coli* involves dynamic redistribution of Min proteins within coiled structures that extend between the two cell poles. EMBO J. **21:**3347-3357.

Shiomi D, Mori H, Niki H. 2009. Genetic mechanism regulating bacterial cell shape and metabolism. Commun Integr Biol. **2(3):**219-20.

Shiomi D, Niki H. 2013. A mutation in the promoter region of *zipA*, a component of the divisome, suppresses the shape defect of RodZ-deficient cells. Microbiol. Open. **2:**798–810.

Shiomi D, Sakai M, Niki H. 2008. Determination of bacterial rod shape by a novel cytoskeleton membrane protein. EMBO J. **27(23):**3081-3091.

Shiomi D, Toyoda A, Aizu T, Ejima F, Fujiyama A, Shini T, Kohara Y, Niki A. 2013. Mutations in cell elongation genes mreB, mrdA and mrdB suppress the shape defect of RodZ-deficient cells. Mol. Microbiol. **87(5):**1029-1044.

Sikdar R, Simmons AR, Doerrler WT. 2013. Multiple envelope stress response pathways are activated in an *Escherichia coli* strain with mutations in two members of the DedA membrane protein family. J. Bacteriol. **195:**12–24.

Singh JK, Makde RD, Kumar V, Panda D. 2007. A membrane protein, EzrA, regulates assembly dynamics of FtsZ by interacting with the C-terminal tail of FtsZ. Biochem. **46(38):**11013-11022.

Spratt BG, Jobanputra V. 1977. Mutants of *Escherichia coli* which lack a component of penicillin-binding protein 1 are viable. FEBS Lett. **79:**374-378.

The Uniprot Consortium. 2014. Activities at the Universal Protein Resource (UniProt). *Nucleic Acids Res* **42:**D191–198.

Thomas PH, Prickett KS, VL, Libby RT, Carl CJ, Cerretti DP, Urdal DL, Conlon PJ. 1988. A short polypeptide marker sequence useful for recombinant protein identification and purification. Nature Biotech. **6:**1204 – 1210.

Tran L, van Baarsel JA, Washburn RS, Gottesman ME, Miller JH. 2011. Single-gene deletion mutants of *Escherichia coli* with altered sensitivity to bicyclomycin, an inhibitor of transcription termination factor Rho. J. Bacteriol. **193:**2229-2235.

Typas A, Banzhaf M, Gross CA, Vollmer W. 2012. From the regulation of peptidoglycan synthesis to bacterial growth and morphology. Microbiol. **10:**123–136.

Uehara T, Park JT. 2008. Growth of *Escherichia coli*: significance of peptidoglycan degradation during elongation and septation. J. Bacteriol. **190:**3914-3922.

van den Ent F, Johnson CM, Person L, de Boer PA, Lowe J. 2010. Bacterial actin MreB assembles in complex with cell shape protein RodZ. EMBO J. **29:**1081-1091.

Varma A, de Pedro M, Young KD. 2007. FtsZ directs a second mode of peptidoglycan synthesis in *Escherichia coli*. J. Bacteriol. **189:**5692–704.

Vicente M, Rico AI, Martinez-Arteaga R, Mingorance J. 2006. Septum enlightenment: Assembly of bacterial division protein. J. Bacteriol. **188(1):**19-27.

Vollmer W, Bertsche U. 2008. Murein (peptidoglycan) structure, architecture, and biosynthesis in *Escherichia coli.* Biochim. Biophysc Acta**. 1778:**1714-1734.

Vollmer W, Seligman S. 2010. Architecture of peptidoglycan: more data and more models. Trends Microbiol. **18:**59-66.

Wagner S, Baars L, Ytterberg AJ, Anja Klussmeier, Claudia S. Wagner, Olof Nord, Per-Åke Nygren, Klaas J. van Wijk and Jan-Willem de Gier. 2007. Consequences of Membrane Protein Overexpression in *Escherichia coli*. Mol. Cell. Prot. **6:** 1527-1550.

Young, KD. 2003. Bacterial shape. Mol. Microbiol. **49:**571-580.

Yousif SY, Broome-Smith JK, Spratt BG. 1985. Lysis of *Escherichia coli* by beta-lactam antibiotics: deletion analysis of the role of penicillin-binding proteins 1A and 1B. J. Gen. Microbiol. **131:**2839-2845.